# NAVAL POSTGRADUATE SCHOOL
## Monterey, California

# THESIS

OPTIMAL ESTIMATION OF TARGET IN CLUTTER
(CHAFF) FROM RADAR

by

Akylas Dim. Katsicogiannis

December 1985

Thesis Advisor:                          H. A. Titus

# REPORT DOCUMENTATION PAGE

| 1a. REPORT SECURITY CLASSIFICATION<br>    UNCLASSIFIED | | 1b. RESTRICTIVE MARKINGS | | | |
|---|---|---|---|---|---|
| 2a. SECURITY CLASSIFICATION AUTHORITY | | 3 DISTRIBUTION / AVAILABILITY OF REPORT<br>Approved for public release;<br>distribution is unlimited | | | |
| 2b. DECLASSIFICATION / DOWNGRADING SCHEDULE | | | | | |
| 4. PERFORMING ORGANIZATION REPORT NUMBER(S) | | S. MONITORING ORGANIZATION REPORT NUMBER(S) | | | |
| 6a. NAME OF PERFORMING ORGANIZATION<br>Naval Postgraduate School | 6b. OFFICE SYMBOL<br>(If applicable)<br>62 | 7a. NAME OF MONITORING ORGANIZATION<br>Naval Postgraduate School | | | |
| 6c. ADDRESS (City, State, and ZIP Code)<br>Monterey, California 93943-5100 | | 7b. ADDRESS (City, State, and ZIP Code)<br>Monterey, California 93943-5100 | | | |
| 8a. NAME OF FUNDING / SPONSORING<br>ORGANIZATION | 8b. OFFICE SYMBOL<br>(If applicable) | 9. PROCUREMENT INSTRUMENT IDENTIFICATION NUMBER | | | |
| 8c. ADDRESS (City, State, and ZIP Code) | | 10. SOURCE OF FUNDING NUMBERS | | | |
| | | PROGRAM<br>ELEMENT NO. | PROJECT<br>NO. | TASK<br>NO. | WORK UNIT<br>ACCESSION NO. |

11. TITLE (Include Security Classification)
OPTIMAL ESTIMATION OF TARGET IN CLUTTER (CHAFF) FROM RADAR

12. PERSONAL AUTHOR(S)    Katsicogiannis, Akylas Dim.

| 13a. TYPE OF REPORT<br>Master's Thesis | 13b. TIME COVERED<br>FROM _____ TO _____ | 14. DATE OF REPORT (Year, Month, Day)<br>1985 December | 1S. PAGE COUNT<br>80 |
|---|---|---|---|

16. SUPPLEMENTARY NOTATION

| COSATI CODES | | | 18. SUBJECT TERMS (Continue on reverse if necessary and identify by block number) |
|---|---|---|---|
| FIELD | GROUP | SUB-GROUP | Microcomputer Radar Simulation |
| | | | |
| | | | |

19. ABSTRACT (Continue on reverse if necessary and identify by block number)
    This work produced a simulation capable of giving the effectiveness
of chaff used in the self-protective mode.  Signal processing techniques
were studied in chaff discrimination in crucial missile conditions.
A missile-ship-chaff model will be constructed to provide the optimum
confusion of the missile.  The radar included in this simulation is a
tracking radar with conical-scan modulation.  Results of simulation runs
illustrate the effects of varying chaff radar cross section when ship
and chaff are in the same resolution cell.

| 20. DISTRIBUTION / AVAILABILITY OF ABSTRACT<br>☒ UNCLASSIFIED/UNLIMITED  ☐ SAME AS RPT.  ☐ DTIC USERS | 21. ABSTRACT SECURITY CLASSIFICATION<br>UNCLASSIFIED | |
|---|---|---|
| 22a. NAME OF RESPONSIBLE INDIVIDUAL<br>H. A. Titus | 22b. TELEPHONE (Include Area Code)<br>(408) 646-2560 | 22c. OFFICE SYMBOL<br>62Ts |

Optimal Estimation of Target in Clutter (Chaff)
from Radar

by

Akylas Dim. Katsicogiannis
Lieutenant, Hellenic Navy
B.S., Greek Naval Academy, 1976

Submitted in partial fulfillment of the
requirements for the degree of

MASTER OF SCIENCE IN ELECTRICAL ENGINEERING

from the

NAVAL POSTGRADUATE SCHOOL
December 1985

ABSTRACT

This work produced a simulation capable of giving the
effectiveness of chaff used in the self-protective mode.
Signal processing techniques were studied in chaff
discrimination in crucial missile conditions.  A missile-
ship-chaff model will be constructed to provide the optimum
confusion of the missile.  The radar included in this
simulation is a tracking radar with conical-scan modulation.
Results of simulation runs illustrate the effects of varying
chaff radar cross section when ship and chaff are in the
same resolution cell.

TABLE OF CONTENTS

LIST OF FIGURES

ACKNOWLEDGEMENT

I wish to express my deepest appreciation to Dr. Hal Titus, for his professional guidance during this work as my thesis advisor.

I would also like to thank my wife Marina for her constant love, care and understanding, my daughter Stellina for never forgetting to say "kiss me, Dad."

# I.  INTRODUCTION

## A.  SEPARATION OF SIGNALS

In many cases we would like to separate two signals from a measurement which is a function of their combination such as their sum.  One of the signals is usually "noise" and the other the "signal" or "information."  Techniques for separating two signals if they have different power spectra are well known; for example, Matched filter and Weiner filter.

The case when two signals have almost the same power spectra must be treated in a different way.  The following are two basic approaches to the problem:

(i)   Use all of the statistical information about the signal to achieve the separation.

(ii) Design measuring techniques such that the two signals will be separable in some sense.

The specific application to be addressed in this research is the tracking radar case where it is necessary to separate a target from chaff.

The objective is to estimate the effectiveness of the chaff in a variety of situations.  Unfortunately, "effectiveness" has nearly as many meanings as there are individuals working on chaff concepts.

Some people are interested in chaff performance only for the first few seconds after dispersal.  Some are concerned

with tracking errors due to chaff and others are interested in multi-target problems in search mode when there are several chaff clouds.

B.  APPLICATION TO TRACKING RADAR

In radar tracking we can have the real target and the false target (chaff) which are in the same resolution cell ($\Delta R$ = Range cell, $\Delta a$ = angle cell). Because of the false target we cannot measure the position of the real target (angles and range). For tracking, we must be able to measure the error in range, azimuth and elevation where the error equals the deviation of the actual target position from the estimated position as given by the midpoint of the resolution cell.

In order to accomplish this, the radar has two windows (gates) for each observable (R, $\theta$, $\phi$). The "weight" of the target in each window is measured by the difference between the normalized weights of each window for each observable. This is used in the calculation to determine target position.

In range we have two gates, the early and the late gates. By measuring the weight of each gate we compute the error in range as:

$$\Delta R = Ro(Veg - Vlg)/(Veg + Vlg)$$

where

$\Delta R$ = The computed error in range

$2\Delta t$ = The width of the range gate

$t_o$ = The position of the range gate (centered at the predicted range from past observations)

$c$ = Velocity of light

$$Veg = \int_{t_o-\Delta t}^{t_o} v(t)dt$$

$$Vlg = \int_{t_o}^{t_o+\Delta t} V(t)dt$$

$V(t)$ = The received signal

The time representation of the range gates and received signals (Veg,Vlg) is given in Fig. 1.1.

When we have two targets in the same resolution cell, the computed error would depend upon the "centroid of gravity" (radar center) of the radar return of the two targets.

Because the two targets have the same (or about the same) power spectral density we cannot distinguish between them by spectral analysis. The object of this research is to estimate the true position of the false target.
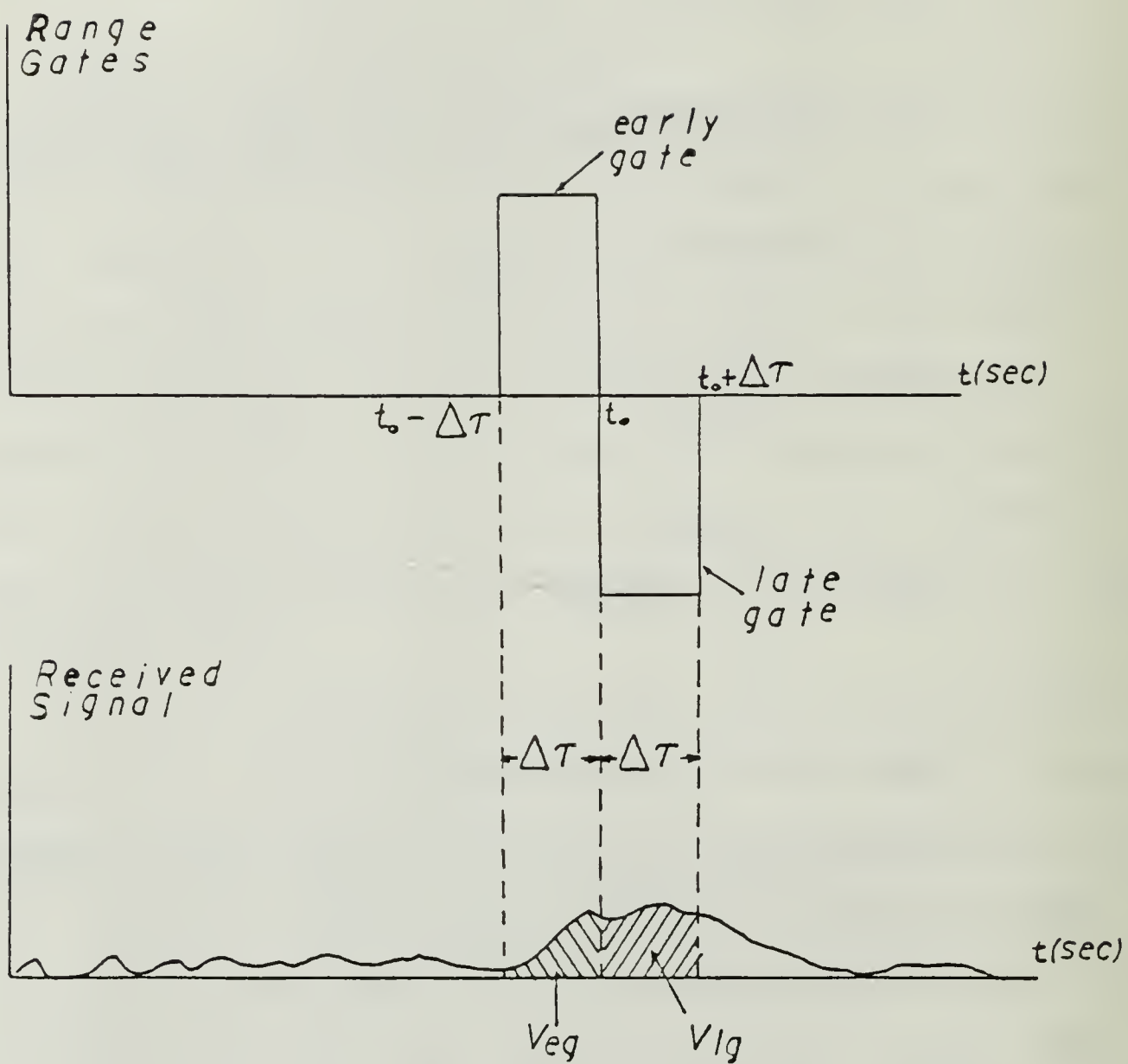
Figure 1.1   Time Representation of the Range Gates and Received
Signals Veg, Vlg

We apply the following constraints:

(i)     An estimator which can be used on missiles, needs
        simple algorithms with the memory size and the
        amount of computation restricted.

(ii)    The size of the antenna is fixed.

(iii)   We will not search for a solution in the r.f. range
        because for each r.f. it is possible to have chaff
        adapted to that frequency.

(vi)    We will restrict ourselves to surface targets which
        imply no reasonable Doppler shift between the target
        and chaff.

# II.   BACKGROUND THEORY

## A.   INTRODUCTION TO TRACKING

A tracking radar system measures the coordinates of a target and provides data which may be used to determine the target path and to predict its future position.  All or only part of the available radar data-range, elevation angle, azimuth angle and doppler frequency shift may be used in predicting future position; that is, a radar might track in range, angle or doppler or any combination.

The function of tracking radar is to select a particular target and follow its course in range, angle and sometimes in doppler frequency.

## B.   TRACKING BY RADAR

Tracking systems can be achieved by two different techniques.

### 1.   Track-While-Scan (TWS)

This method of tracking basically uses data from search radar.  The idea is to take an observation of the target each time that the antenna sweeps by the tracked target.  This tracking class is not of interest in this study.

### 2.   Continuous Tracking Radar

In this method of tracking, the antenna is always directed at the target due to action of the control system.

14

There are several methods of tracking (i.e., methods of generating the error signals to close the off boresight antenna position). The important methods are:

(i) Conical scan (Cs)

(ii) Monopulse

Those methods are distinguished by their difference in angle tracking. The principle of range tracking is almos the same for all radars. Since the most accurate and interesting case is the conical scan, we will concentrate on it and after will give the theory of the other techniques in summary.

3. Angle Tracking

a. Conical Scan

In a conical scan system, angles are measured by a single antenna, whose radiation pattern rotates periodically about a certain axis as shown in Fig. 2.1. When the target is in the axis direction, the radar will have a constant return signal. The coordinates of the off axis target is determined on the basis of comparison to the envelope of received signals with a reference signal. For this reason we cannot measure the error in one pulse but we have to wait at least one period of antenna scan to get the information. A block diagram of the C.S. system is given in Figure 2.2. The antenna A scans in space with angular frequency $w_s$. Two references for the phase detector are generated by the antenna (Az and El). The position of the

15
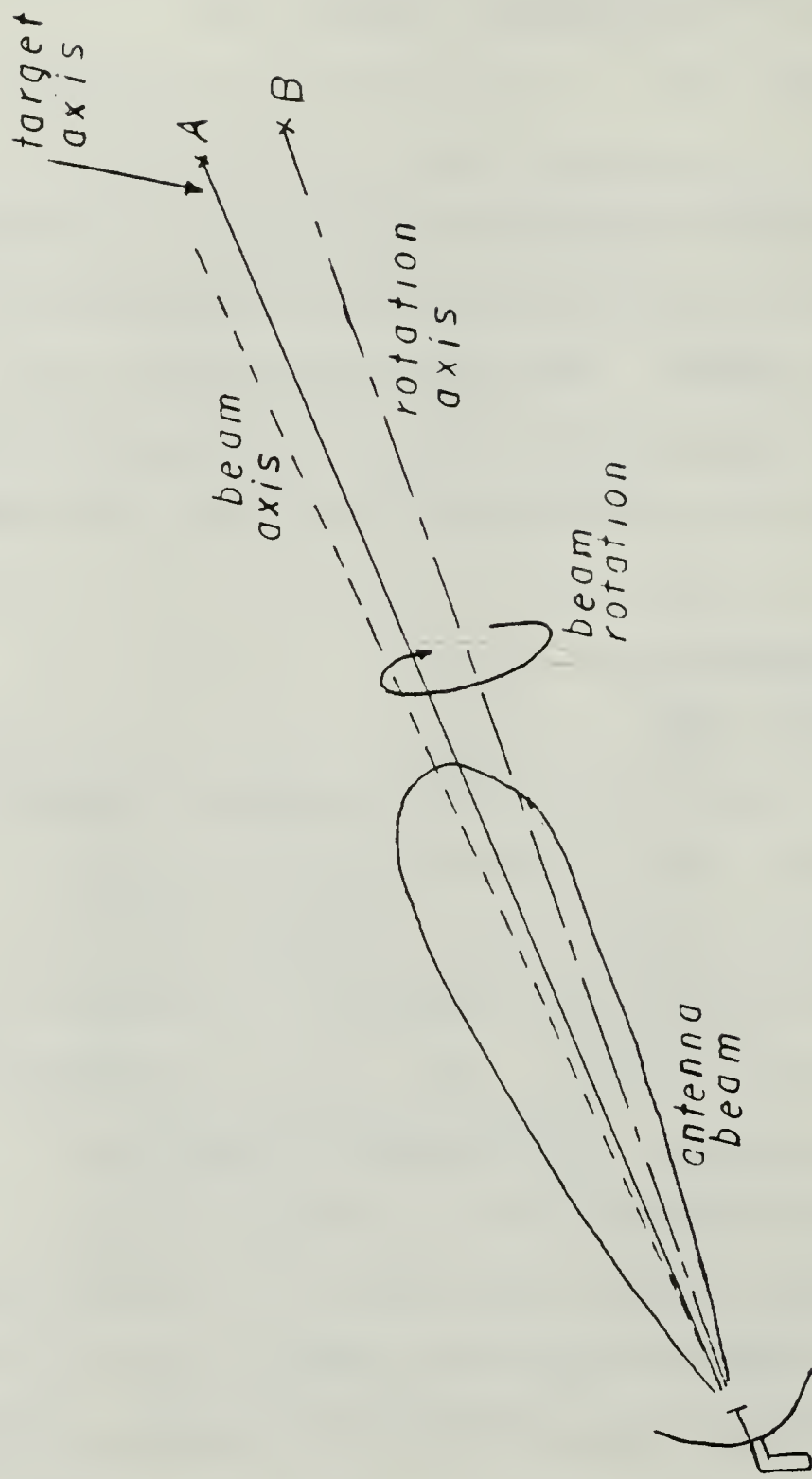
Figure 2.1  Conical-Scan Radar Tracking
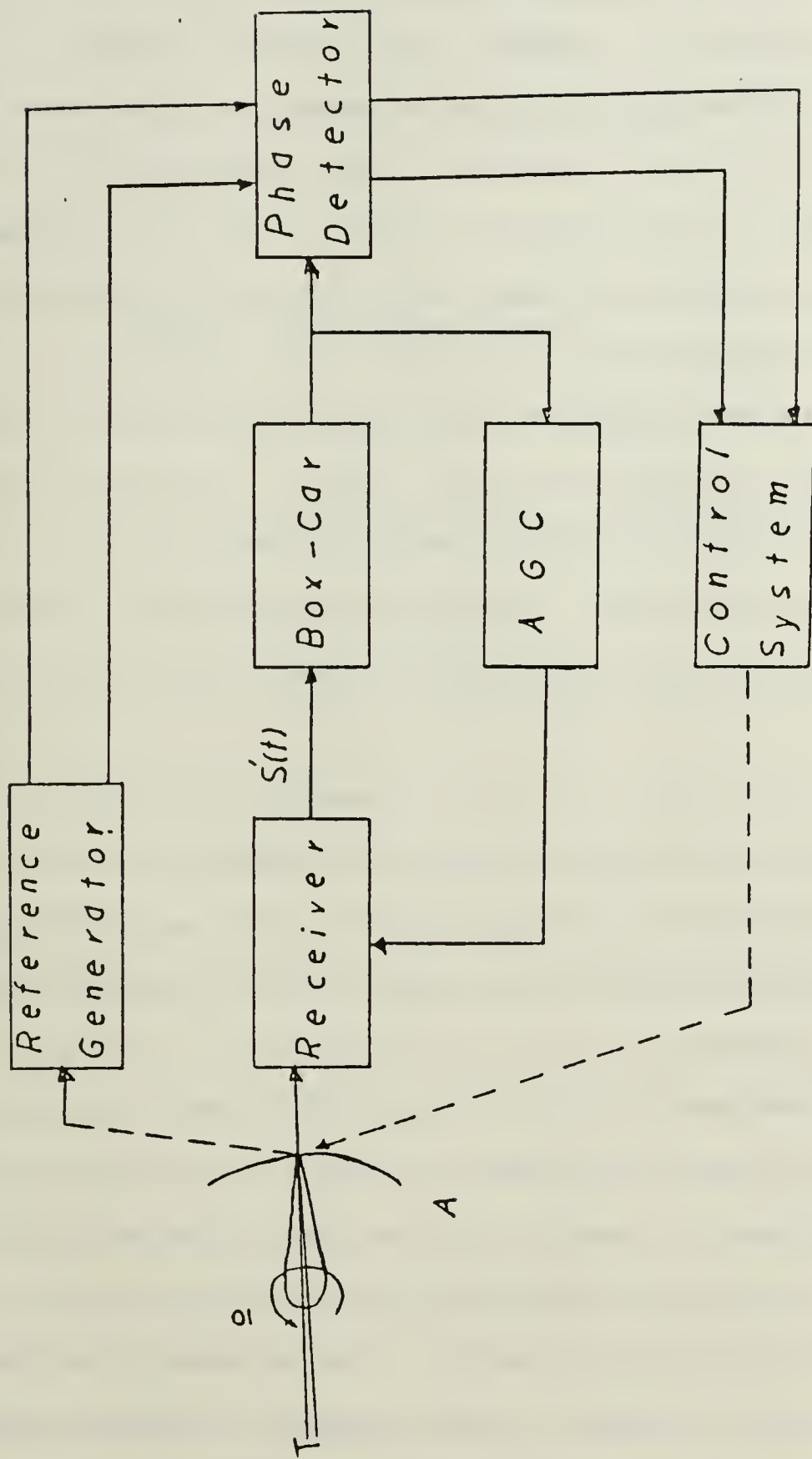
Figure 2.2  Block Diagram of Conical-Scan (C.S.) System

antenna is controlled by the control system. Assume one
target at position T. Because the target is assumed to be
off the axis of rotation, the echo signal will be modulated
at frequency $w_s$ (C.S. frequency). The amplitude of the
signal depends on the position of the target with respect to
axis of rotation and the phase will depend on the direction
of the angle between the target and rotation axis.

When the antenna is on the target we will get
zero modulation at the receiving signal. The modulation
pulses pass through a receiver which is controlled by an AGC
(automatic gain control). The signal then passes through a
"box-car" circuit which changes the amplitude modulated
pulses).

The outputs from the phase detectors (for Az and
El) are the errors in El and Az and by using these errors we
can close the loop on a control system which will move the
antenna to reduce the error to zero, so the antenna "looks"
towards the target.

Because we would like to have the same amount of
error for the same error angle, independent of the target
and range we have to measure the modulation index. The
method which is usually used to achieve this objective is
the AGC (automatic gain control). The purpose of the AGC is
to make the average power to be a constant. This can be
accomplished by controlling the gain of the receiver.

The signal can be represented by:

$$S(t, \theta_\tau) = C[1 + m(\theta_\tau) \cos(w_s t + \phi c)]$$

where

$m(\theta_\tau)$ = modulation index

$w_s$ = conical scan frequency of the antenna

$\phi c$ = phase of signal relative to C.S. frequency

$C$ = known constant

$\theta_\tau$ = the position angle of the target

b.   Monopulse

A monopulse radar system is a tracking system that derives all its tracking error information from a single pulse.  In addition, new and independent error information is generated with each new pulse.

The basic principle of monopulse radar is that of combining the R.F. circuits of two antennas to obtain simultaneously both sum and different signals.

Physically two antennas are not necessary since the "arithmetic" can be accomplished with a single parabolic reflector and two radiators, or "feeds", displaced from the focal point of the antennas.

The difference signal provides the magnitude of the angle error while the sum signal provides the reference to extract the sign of the error signal. The sum signal also provides a means of extracting the radar range measurement as in a conventional pulse radar.

When we want two-coordinate information (azimuth and elevation) then four antenna feeds are required to provide the sum and difference.

4.  Range Tracking

The most widely used technique for tracking in range is based on two range gates. There are no special techniques for the method of angle tracking. Information about the range is taken, in most of the cases, from the sum channel in the monopulse radar and from the incoming pulses in C.S. As target speeds increase, it is difficult for an operator to perform at the necessary levels of efficiency over a period of time and automatic tracking becomes a necessity.

We will briefly cover the principle of automatic range tracking. The technique for automatically tracking in range is based on the idea of opening two gates before and after the estimated time of the center of arrival of the pulse ($t = 2R/c$, $R$ = target range, $c$ = velocity of light). One is the early gate (g1), and the other is the late gate (g2). The echo signal, position of the gates at particular instants and error signal are shown in Fig. 2.3.
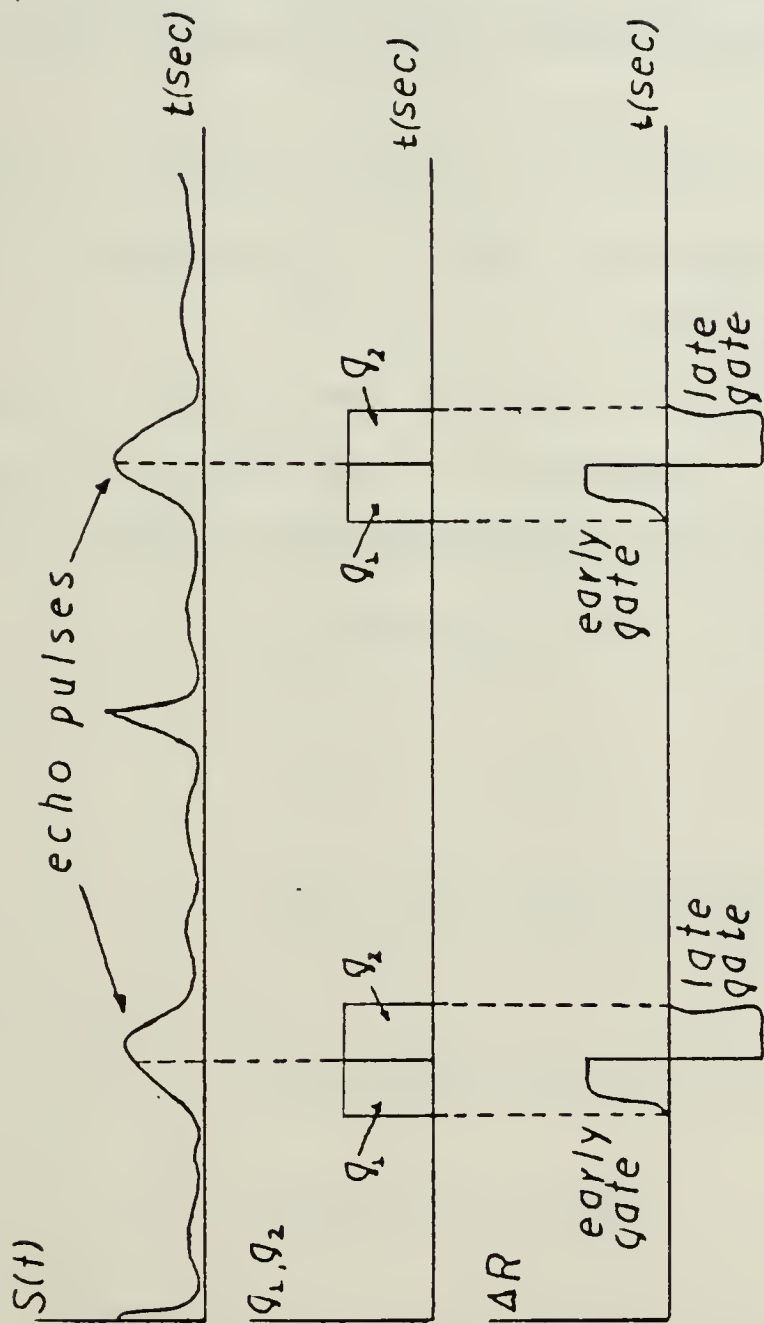
Figure 2.3   Echo Signal, Position of the Gates and Error Signal

21

The portion of the signal contained in the early
gate substracted from the portion of the signal contained in
the late gate produces an error signal.  The magnitude of
the error is a measure of the difference between the center
of the pulse and the estimated range which is the center of
the two gates.

The error is fed into a control system to estimate
the range and when the error signal is zero, the range gates
are centered on the pulse.

Because we want to have the same output error, $\Delta R$
for all the targets, independent of the target, we must
normalize the pulses, and this is done by AGC which has
already been applied in angle tracking.

## III. STATEMENT OF THE PROBLEM

A. INTERFERENCE CAUSED BY TWO TARGETS

Let's consider the problem of tracking when a false target is in the same resolution cell, i.e.,

$$\Delta L/R < \theta_{3db} \qquad \Delta R < c\Delta t/2$$

where:

$\theta_{3db}$ = the beamwidth of the antenna (in radians)

$2\Delta t$ = pulse length

R = range of target

$\Delta L$ = the difference between the true target and the false target perpendicular to the line of sight of the antenna

$\Delta R$ = the difference between the true target and the false target in range

c = velocity of light

For simplicity, let us consider the two dimensional case only (range and elevation). The principle in three dimensions is the same but more complicated, and the results can be obtained by a straightforward extrapolation of the

23

two-dimensional case. We will consider the case of point

targets for developing the theory, but we will implement the

results when the targets have complex structure.

B.   INTERFERENCE IN ANGLE CREATED FROM TWO TARGETS

Changes in the target aspect with respect to the radar

can cause the apparent center of radar reflections to wander

from one point to another. In general, the apparent center

of reflection might not correspond to the target center.

The angular fluctuations produced with small targets at long

range may be of little consequence in most instants.

However, at short range or with relatively large targets (as

might be seen by a radar seeker on a homing missile),

angular fluctuations may be a chief factor limiting tracking

accuracy. Angle fluctuations affect all tracking radars

whether conical-scan or monopulse.

Consider the case of two point targets in the same

resolution cell of the radar with spacing $\Delta L$ (i.e., $\Delta L/R <$

$\theta_{3db}$, $\Delta R < c\Delta t/2$). As the relative path lengths between the

radar antenna and the two sources vary (i.e., R1 and R2),

the two signals will alternately add and substract, and so

the amplitude and phase of arrived signals will change.

Although such a simple situation (two point targets) may be

fictitious, it will illustrate the main behavior. The

relative amplitude between the RCS (Radar cross section) of

the two targets is assumed to be a constant "A" and the

relative phase difference also constant, "a". The

difference in phase is due to difference in range ($\Delta R$) or to

reflecting properties. The relative angular error ($\Delta\theta/\theta_o$)

is given by [Ref. 1].

$$\Delta\theta/\theta_o = [A^2 + A\cos(a)]/[1 + A^2 + 2A\cos(a)]$$

The position of the stronger target corresponds to

$\Delta\theta/\theta_o = 0$, while the smaller target position is at $\Delta\theta/\theta_o = 1$

as in Figure 3.1.

The position of the tracking system depends on the

relative phase "a" and the ratio "A". One can show that for

$0 \le A \le 1$ and $0 \le a < 2n$ the values of $\Delta\theta/\theta_o$ will be

between:

$$-\infty < \Delta\theta/\theta_o \le 0.5$$

When the echo signals are in phase, the error reduces to

A/(A+1), which corresponds to the so-called "center of

gravity" of the two targets.

Now, when we have a complex target, such as a chaff or a

ship, the ratio "A" is a random variable which changes from

pulse to pulse. Taking these into the given servo loop of

the radar system, one can compute the statistics of the ran-

dom variable $\Delta\theta$, and this can give us a good approximation
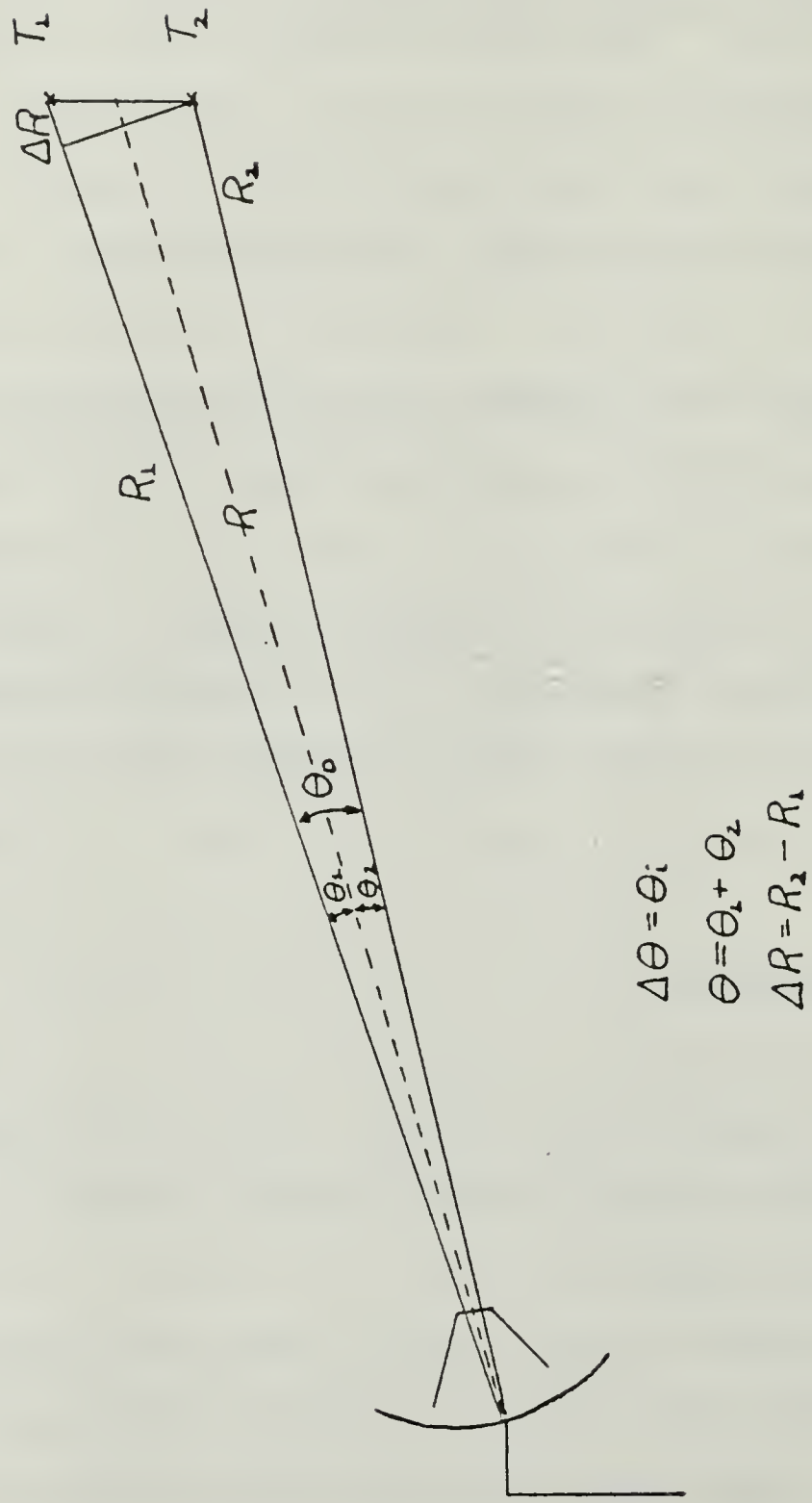
Figure 3.1  Geometric Representation of the Problem

of the error (for example, mean and variance) caused by the addition of two targets in the same resolution cell.

However, the simple case results are sufficient for our problem, to show that the results of two target returns in the same resolution cell causes an error in the estimation of the position of the true target which depends on the signal ratio between the two targets. When the two targets have a complex structure rather than a point, the results are much more complicated and we have to take into account the circuits involved and the statistics of the target's returns.

C.  CONCLUSION

In the last paragraph we have studied that when there is an additional target in the resolution cell, the radar will not track on either of the targets, but on their center of gravity. In order to eliminate this phenomemon, we must change the design of the radar so that it will track on two targets. There are two main ways for accomplishing this objective:

 (i)   Extract information of the location of the target by processing the signal after the receiver.

 (ii)  Modify the receiver and the filtering process after the receiver in order to extract the information of the two targets.

We will consider later the case of a ship as the true target and the chaff as the false target.

## IV.  COATED DIPOLES AS CONFUSION REFLECTORS

A.  CHAFF

Chaff is defined in standard dictionaries as husks of grain or anything useless.  Chaff is now a general term that is defined as follows:  Elemental passive reflectors, absorbers or refractors of radar which can be floated or otherwise suspended in the atmosphere or exoatmosphere for the purpose of confusing screening or otherwise adversely affecting the performance victim missile system.  Examples are:  metal foils, metal coated dielectrics (aluminum, silver and zinc on nylon or glass), aerosols and semiconductors.

Chaff can be manufactured to be effective over wide frequency ranges.  It does not depend on a prior knowledge or detailed information about victim missile systems.  Also when properly deployed, it is effective against many radars simultaneously.  These two facts produce tremendous advantage when planning to defend a ship against a complex of radar and missile systems that are being continually updated.

### 1.  Chaff Materials

During the early years, after the Second World War, aluminum foils cut into strips were still widely used and

are still one of the principal types of the chaff material today. The more recent types include aluminum coated glass filaments developed by Bjorksten Research Laboratories in the USA and silver-coated nylon monofilament developed by Cherming [Ref. 3]. These three types constitute the majority of chaff materials being manufactured today and described in more detail.

Basic properties of the three principal chaff types are given in Table I. The great majority of silver-coated nylon aluminized glass is produced with the nominal diameter shown for each type. Three types of aluminum chaff and the differences of these filaments are shown in the first column of Table I. They have an effect on the chaff motion and hence, radar response of the dipoles.

The composition and characteristics of each type are described below.

a. Silver-Coated Nylon

Silver-coated nylon consists of a thin deposit of silver or nylon monofilament. Long dipoles ($\approx$ 50 mm) tend to show an exaggerated zig-zag motion, but the descent is still predominantly horizontal. Because of this flight attitude, in the long term, a chaff cloud formed with silver-nylon dipoles will show a strong reflection of horizontally polarized waves but appreciably lower vertical-polarization response. In the first few seconds after

29

TABLE I

COMPARISON OF PHYSICAL PROPERTIES OF COMMON CHAFF TYPES

| Type | Nominal section dimensions of filaments | Density of material (1) | Normal maximum packing density (2) | Normal maximum bulk density (1) × (2)/100 | Mean fall rate in still air at sea level | Ratio of number of dipoles per unit volume of payload (silver nylon = 1) |
|---|---|---|---|---|---|---|
| | μm | kg/m³ | % | kg/m³ | m/s | |
| Aluminised glass | 25 | 2550 | 55 | 1403 | 0.30 | 10.97 |
| Silver coated nylon monofilament | 90 | 1300 | 65 | 845 | 0.60 | 1.00 |
| 2 × 1 aluminium foil | 50 × 25 | 2700 | 55 | 1485 | 0.40 – 0.45 | 4.31 |
| 4 × 1 aluminium foil | 100 × 25 | 2700 | 55 | 1485 | 0.50 – 0.55 | 2.15 |
| 8 × 1/2 V-bend aluminium foil | 200 × 12 | 2700 | 45 | 1215 | 0.50 – 0.55 | 1.84 |

30

deployment, this polarization effect is not significant because of turbulence induced by the dispensing system. Silver-nylon has two disadvantages; it is fairly expensive material and also cannot normally be manufactured in diameters smaller than the nominal 90 mm. Therefore the number of dipoles in a given payload space will be less than most other materials, and the theoretical radar cross-section of the chaff could will be lower.

However, a silver-nylon chaff has the least tendency of all chaff materials to birdnest, and this, to some extent, compensates for the lower numbers of dipoles per unit volume especially at low frequencies. The major disadvantages of silver-nylon are its low bulk density and robustness. The dipoles can withstand large dispensing forces and suffer little or no permanent distortion.

b. Aluminum Foil

Aluminum foil chaff is produced by shredding reels of foil into filaments whose length is equal to the width of the original reel of foil. The shredding process causes a regular series of twists to be put into the filament length, and hence dipoles produced from these filaments are also twisted. This gives aluminum foil chaff types their distinctive flight motion.

The predominant flight mode of 4 x 1 aluminum is termed helicopter motion, and as the name implies, the

dipoles descend with rapid rotation in the horizontal plane. The comments regarding horizontal and vertical polarization made for silver nylon also apply to 4 x 1 aluminum.

Spiral motion occurs principally in 2 x 1 aluminum, and the dipole descends at an angle usually between 15 and 60 to the horizontal in a slow spiral without tumbling or rapid rotation of the dipole itself. Because of the large vertical component in the flight motion, 2 x 1 aluminum is used a great deal in naval applications, where the chaff cloud may be required to retain a high degree of omnipolarized response for some time. This is illustrated later, where relative responses in horizontal and vertical polarization are compared for 2 x 1 aluminum and aluminized glass.

Lead particles suspended in a lacquer can be applied in stripes running along the length of a reel of foil. When shredded and cut to dipole lengths compatible with the original stripe spacing, dipoles are produced with the lead stripe at one end. However, this type of chaff is no longer commonly used and has been superseded in some cases by 2 x 1 aluminum.

The distinctive feature of 8 x 1/2 aluminum foil chaff is its V-section. The dipoles are bent mid-way across width, and the bend extends along the length of the dipole. This bend is put in during the shredding process and results

32

in long 8 x 1/2 dipoles being more rigid than 4 x 1 or 2 x 1
dipoles of corresponding length.  Therefore, 8 x 1/2
aluminum is most useful for low-frequency dipoles.

c.  Aluminized Glass

Aluminized glass is the slowest descending chaff
of all the common types, and its small diameter means that
the number of dipoles per unit volume of payload space is
very large compared with silver-nylon or the aluminum foil
types.  The flight motion is basically horizontal, because
the dipoles are cylindrical in section with no major
distortions.  However, the section is not so regular or
smooth as silver nylon, and dipoles sometimes have a slight
degree of spiral as a result of the manufacturing process.
Therefore, the average vertical polarization response per
dipole is greater than with silver-nylon, but not so great
as a 2 x 1 aluminum.

d.  Other Materials

Other types of chaff material include zinc-
coated glass filaments and copper-coated polyestor filament.
Zinc is about 4-5 times as resistive as copper and is,
therefore, near the lower limit for consideration as an
efficient scattering material.

Copper plating of large quantities of fine
filaments is an expensive process compared with shredding
aluminum foil or aluminum-coating glass filaments, and the

33

resultant chaff offers no significant advantages over the
more common chaff types.

Carbon or graphite fibers are difficult to coat
with metals and in themselves are too resistive to act as
efficient scatterers.

While other new chaff materials will certainly
be developed, there is scope for improvement of manufac-
turing processes for the current materials.  It is important
to improve the efficiency with which the available materials
are used, e.g., reduction of amount of dispensing, reduction
of the time to achieve maximum RCS (Radar Cross Section) and
the investigation of ways of dispensing which allow cheaper
and more efficient deployment.

B.   PRINCIPLES OF MICROWAVE REFLECTION BY CHAFF

The general philosophy of using bundle chaff to confuse
a radar is that chaff bundles should be dispensed at a rate
such that there will be less than the victim radar range
cell distance between successive bundle blooms or a near
continuous dipole field within each victim radar angle cell
or antenna beamwidth.  This philosophy is generally true
when chaff clouds present false target at relatively large
distances away from a friendly ship to be protected.

An important consideration is J/S where J is the signal
reflected by the RCS of the chaff and the S is the RCS
(Radar Cross Section) signal from a target within the chaff

cloud or being protected by chaff bundles. Generally, the ratio J/S should be greater than three db for successful chaff protection.

1.  Radar Cross Section

Chaff consists of electrically conducting filaments which are cut to form dipoles that are resonant at particular wavelengths. When chaff is ejected into the atmosphere, the maximum theoretical RCS (Radar Cross Section) size corresponding to the total number of ejected dipoles is never achieved. In fact, only a minority of the dipoles dispensed become effective as reflector confusion to the victim radar. Randomly oriented dipoles with respect to the direction of incident electromagnetic wave have average cross section ($\sigma$) [Ref. 2]:

$$\sigma = .18\lambda^2 N$$

where

$\sigma$  = the cross section in sq. meters

$\lambda$  = wavelength in meters

N  = number of effective dipoles

The average single dipole cross section versus frequency for random orientation is shown in Fig. 4.1. The
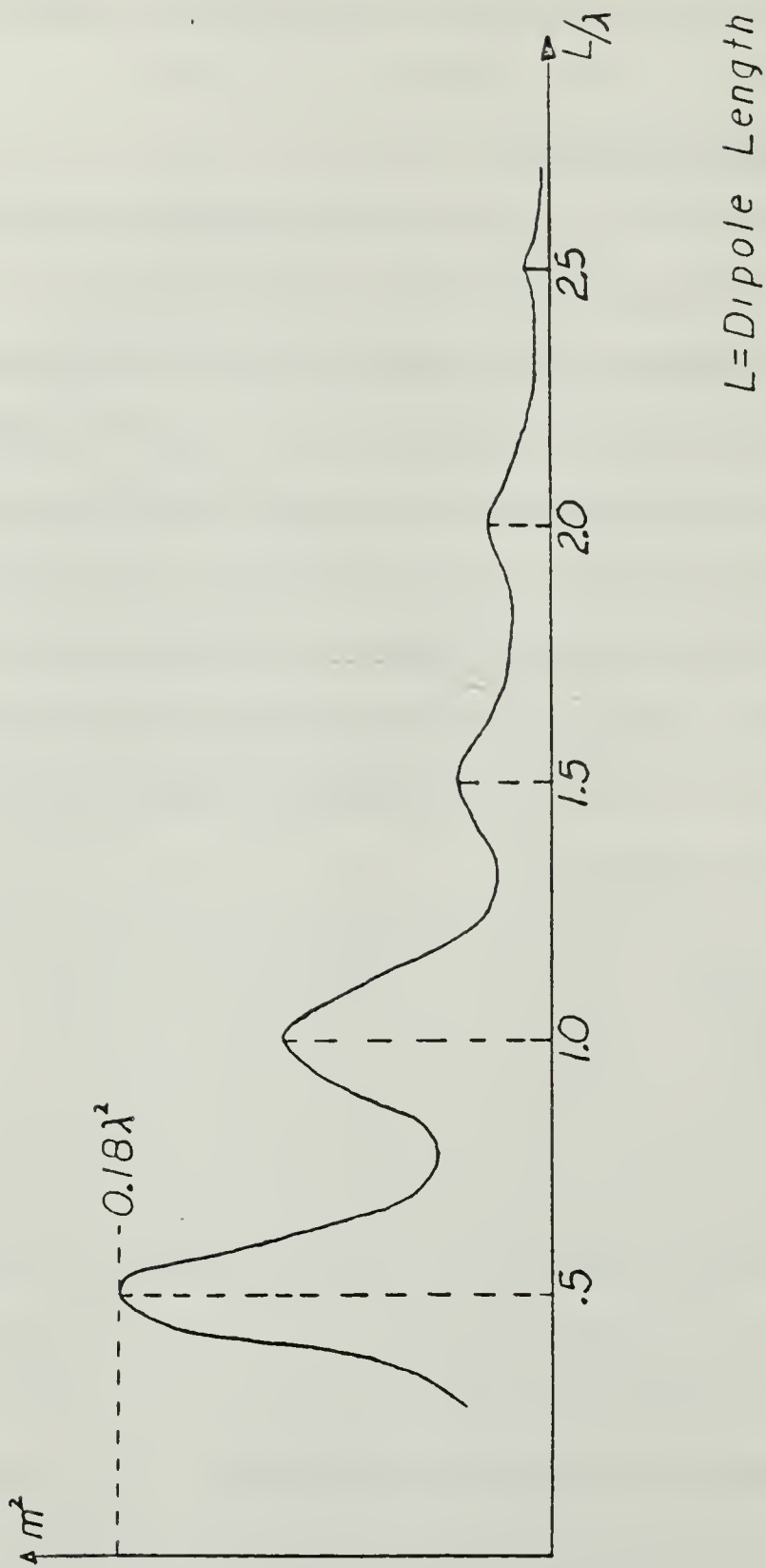
35

Figure 4.1  Average Single Dipole RCS Graph

maximum cross section occurs when the chaff particle is less
than 1/2λ long.  This is because the electromagnetic wave
travels more slowly in the dipole material than in free
space.  The physical half wavelength becomes shorter as the
width or diameter of the conductor increases in proportion
to the length.  The ratio A, of length to diameter or width
of dipoles has to be taken into account when computing the
resonant frequency.

So for cylindrical dipoles [Ref. 3]:

$$A = L/d$$

where:

d = the diameter of dipole

L = the length of dipole

For rectangular section dipoles [Ref. 3]:

$$A = 4L/w$$

where

w = the dipole width (the largest dimension of the
dipole end section)

The variation of dipole length as a fraction of the
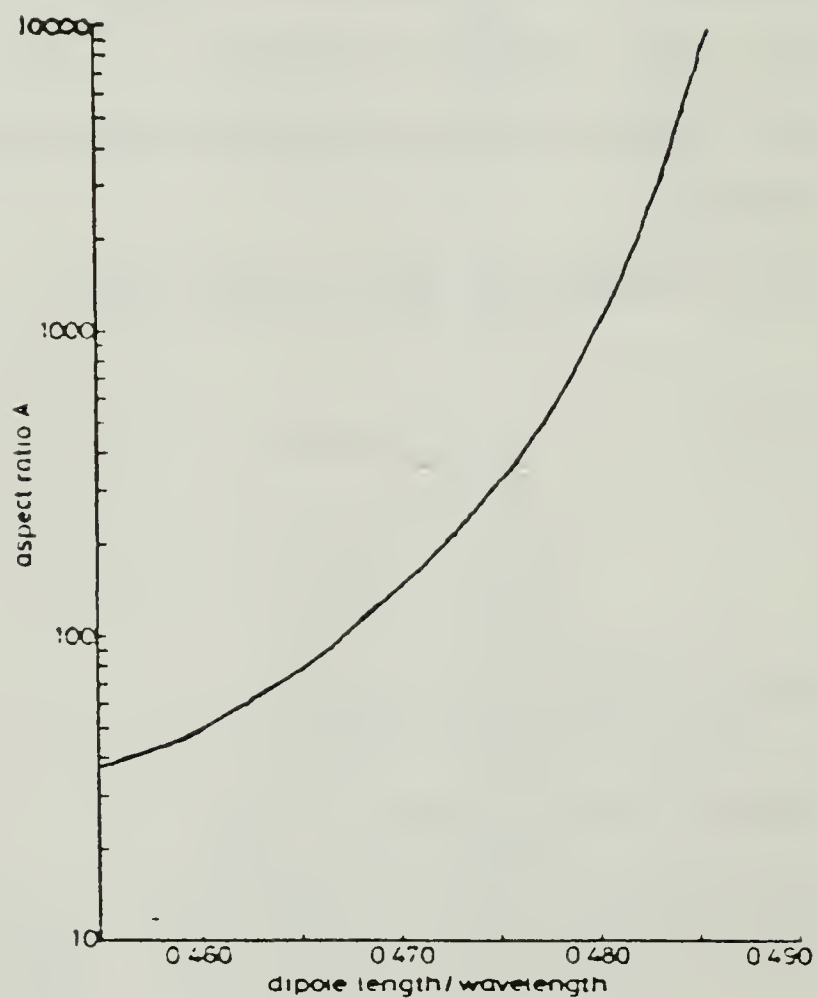wavelength against the aspect ratio is shown in Fig. 4.2.

37

Figure 4.2   Variation of Dipole-Length/Wavelength with
             Dipole Aspect Ratio

The conductive coating of the cylindrical dipole should have a radius which is large compared with the skin depth, and the conductive coating thickness should be at least equal to the skin depth to RF resistance. The requirement for low RF resistance has tended to limit the choice of metals to aluminum, silver, copper, or zinc. Because of its low cost and high conductivity, aluminum is the most used material.

A chaff filament will have its largest effective RCS (Radar Cross Section) at its dipole resonant frequency but will show significant levels of response when it is a full wave resonator and at further multiples of the half wavelength.

When forming a chaff pack, the harmonic peaks must have the required frequency band. The bundle is said to have purity if all of the dipoles are of single length alternatively, the bandwidth of the chaff bundle can be broadened, almost arbitrarily with an approximate mix of lengths in a single bundle. Another bandwidth broadening approach is to dispense multiple bundles, each cut for different frequencies.

With metallic foil or metal coated, a dielectric dipole will reflect a signal back to the radar which has a randomly modulated frequency bandwidth with less than plus or minus about 100 Hz around the carrier frequency of radar.

## 2. Operational Consideration

When chaff is dispensed, it grows in few tenths of a second up to several seconds, depending on the type of the dispenser used. At high altitudes the chaff will fall faster than at lower altitudes because of the thickness of the air. The average fall rates are roughly about 250 ft per minute for fine foil-type dipoles. The fine metal-coated dielectric dipoles, sometimes called angel hair, can fall much more slowly and even rise in altitude under usual conditions.

One individual unit of dispensing chaff is called a packet, muffin, cylinder, or bundle. Many hundreds of thousands of dipoles can be contained in one bundle of metallic-foil chaff or many millions in a bundle of metallic-coated dielectric chaff.

The polarization of chaff can change as the dipoles fall. Some dipoles will have a tendency to remain approximately horizontal and some will remain vertical. Depending on the environment of conditions, the top portion of the chaff cloud may have a tendency for reflecting horizontally polarized waves and the lower portion may have a tendency for reflecting vertically polarized waves.

When a beam of radar illuminates an area of chaff cloud it receives the largest reflected energy from the dipoles that are located on or near the surface of that

area.  The dipoles nearest the radar will disperse the
portion of the radar energy which these intercept in all
directions, so reducing the incident radar energy before it
impinges on these dipoles in the chaff cloud that is farther
from the radar.  The reflected energy from these dipoles
will be dispersed in the same manner.  Therefore, all the
effective dipoles dispensed are not equally effective
against a single radar.

A target beyond a chaff cloud should appear smaller
to the radar because the radar signal experiences an
effective attenuation during each of two traversals of the
chaff cloud.  So using conventional metallic dipoles,
density of cloud must be extremely high for low values of
attenuation.

### 3.  Chaff Applications

Chaff in Naval use is most commonly ejected from
rocket shell or mortar systems.  Naval rockets can contain
up to 7 kg of chaff, and mortar systems typically dispense
up to 3 kg of chaff from several grenades fired simul-
taneously.  There are three main modes of use for chaff at
sea.

### a.  First Mode

This is known as distraction decoy dispensed by
rockets and shells at ranges up to 2 km from the vessel, and
a pattern of several rockets fired in different directions

is used to provide alternative targets to missiles, which are still at some distance from the vessel.

   b.   Second Mode

   This is known as the dump mode; it is used closer to the vessel (less than 1 km away) where it works as passive ECM (Electronic Counter Measure) to deny range information to the seeker and is used in conjunction with chaff fired from a rocket as false target to the attacking missile.

   c.   Third Mode

   This is known as the centroid mode, used very close to the ship where the chaff cloud is dispensed at a range of 100-400 m.  A large echoing area must be realized in a few seconds of firing and the chaff cloud appears initially near the ship.  After the ship goes out and away from the chaff echo the missile becomes confused, avoiding the true target.  The centroid mode is achieved with rockets or mortar systems and is a tactic which will succeed best with vessels of relatively small RCS (Radar Cross Section) such as converts or other ships.

   In Naval uses, multipath effects can be used with advantage where the free-space RCS of a chaff cloud is greatly enhanced by its proximity to the sea.

   Various techniques are employed in Naval dispensers to decrease the time required for a chaff cloud

42

to achieve maximum RCS, and in the case of self-protection applications for ships, the mechanisms to dispense the chaff have become quite sophisticated.

## C. CONCLUSION

The task of discriminating between chaff and the target that it is intended to protect may appear to be easy, especially with the increasing sophistication of modern radars and signal processing techniques. There are several factors which, taken together, justify the existence of chaff and promote its use:

(i)   Improved dispensing systems and the tactics used with them, have counterbalanced the improvements in radar systems with regard to chaff discrimination.

(ii)  If the chaff can be discriminated from real targets, the discrimination process itself means that valuable time is spent by a computer system. So the presence of chaff echoes must degrade the overall performance of the system.

(iii) Chaff is a cheap electronic countermeasure. Chaff dispensers are, in themselves, relatively low cost items compared with, for instance, an active jamming. The ammunition for the chaff dispenser is also a low cost item when compared with maintenance and repair of an active system.

(iv)  It is difficult to produce large radar echoes at a great distance from a vessel under command from that vessel except by the use of chaff dispersed from a rocket or shell.

While other decoys may be developed, chaff dispensing is currently far more efficient and cost effective in this regard than any other technique.

43

## V.   CONICAL-SCAN MODULATION

The effect of conical scanning is to multiply the complex envelope of the echo signal from a target not on the boresight of the radar by a modulation function $m(t)$ that is periodic at the scan frequency $f_s$.

The X-band radar used to collect chaff data employs conical scanning to generate error signals for the control system which maintains the beam on target. Unfortunately, the statistics of the received signal are modified by the modulation induced by this scanning.

This section discusses the effect of conical-scan modulation on the echo signal from a chaff cloud; in particular one expression is given that shows how the spectral density is modified by the modulation. Fortunately in this study, conical-scan modulation has only a slight effect on spectral density.

Suppse $z_m(t)$ and $z(t)$ are the complex envelope of the echo signal when conical-scan modulation is and is not present respectively.

Assume that (1) all dipoles lie within the mainlobe of the antenna pattern and (2) the phase of the antenna is constant across the mainlobe. Under these assumptions the modulation function will depend on the transmitted beam

44

pattern, the scan rate and the positions of the dipoles
relative to the rotation axis.

In the apendix, it is shown that [Ref. 4]:

$$z_m(t) = m(t) \ z(t)$$

where the modulation function m(t) may be approximated by an
expression of the form:

$$m(t) = Mo + BMo \cos(2nf_s\tau + a)$$

where

$\quad$ B $\quad$ = estimated amplitude data for a chaff data set

$\quad f_s \quad$ = scan frequency

$\quad$ Mo,a = unknowns

The autocorrelation function of $z_m(t)$ obtained by time
averaging is then [Ref. 4]:

$$Rz_m(\tau) = \overline{z_m(t + \tau) z_m(t)}$$

$$= Mo^2 + (Mo^2 B^2/2) \cos(2nf_s\tau)\} Rz(\tau) \qquad (5-1)$$

where $Rz(\tau)$ is the autocorrelation function of $z(t)$.

45

Taking the Fourier transform of both sides of (5-1) gives the relationship between the spectral densities of $z_m(t)$ and $z(t)$ [Ref. 4]:

$$Sz_m(f) = Mo^2 Sz(f) + (Mo^2 B^2/4) Sz(f-f_s) + (Mo^2 B^2/4) Sz(f+f_s)$$

(5-2)

So $Sz_m(f)$ is the sum of three terms as follows:

a) First term is $Mo^2 Sz(f)$

b) Second and third terms are $(Mo^2 B^2/4) Sz(f-f_s)$ and $(Mo^2 B_2/4) Sz(f+f_s)$ shifted by $-f_s$ and $+f_s$ respectively.

Let $n_m(f)$ and $n(f)$ denote the normalized unity area frequency density functions corresponding to $Sz_m(f)$ and $Sz(f)$ respectively; then [Ref. 4]:

$$n_m(f) = (1-2b)n(f) + bn(f-f_s) + bn(f+f_s)$$

(5-3)

where:

$$b = B^2/(4 + 2B^2)$$

Of particular interest is the effect of conical scanning on the mean $v_o$ and standard deviation $\sigma_v$ of the velocity density function $q(v)$.

Letting $q_m(v)$ and $q(v)$ denote the density functions with and without conical-scan modulation respectively obtained from (5-3), the relationship:

46

$$q_m(v) = (1-2b)q(v) + bq(v+v_s) + bq(v-v_s) \qquad (5-4)$$

where:

$$v_s = -\lambda f_s/2$$

Using (5-4) it may be shown that the variance of $q_m(v)$ is:

$$\sigma_{vm}^2 = \int_{-\infty}^{\infty} (v-v_o)^2 q_m(v)\,dv = \sigma v^2 + 2bv_s^2 \qquad (5-5)$$

where:

$$\sigma_v^2 = \int_{-\infty}^{\infty} (v-v_o)^2 q(v)\,dv$$

Rearranging (5-5) we obtain a simplification for the standard deviation of the velocity density function.

$$\sigma_v = k\sigma_{vm}$$

where

$$K = (1-2bv_s^2/\sigma_{vm}^2)^{1/2}$$

An expression for the error in $\sigma_v$ due to conical-scan modulation is [Ref. 4]:

47

$$e\sigma = \sigma_{vm} - \sigma_v = (1-k)\sigma_{vm}$$

Finally, define the conical scan distortion ratio Ds as [Ref. 4]:

$$Ds = b/(1-2b) = B^2/4$$

so that Ds is the ratio of the heights of the shifted components in $n_m(f)$ introduced by conical scanning to the height of the unshifted component.

Following is an example given as part of this section to show the spectral density Sz(f) when conical-scan modulation is present.

A. EXAMPLE

It is desired to use the amplitude data A = 0.12 for a given chaff data set and normalize it so that $\bar{a}_m$ = 1.0. Since A and $\bar{a}_m$ are known, B may be estimated also; thus $B = (2A/\bar{a}_m)^{1/2} = 0.49$.

A plot of autocovariance Cam($\tau$) for the given data set where conical-scan modulation is present is shown in Figure 5.1. Taking the Fourier transform of autocovariance function yields the corresponding spectral density Sam(f) as shown in Figure 5.2. In this case (given chaff data) the spectral density is very narrow so it is possible to the main peaks and the two secondary peaks predicted by (5-2).
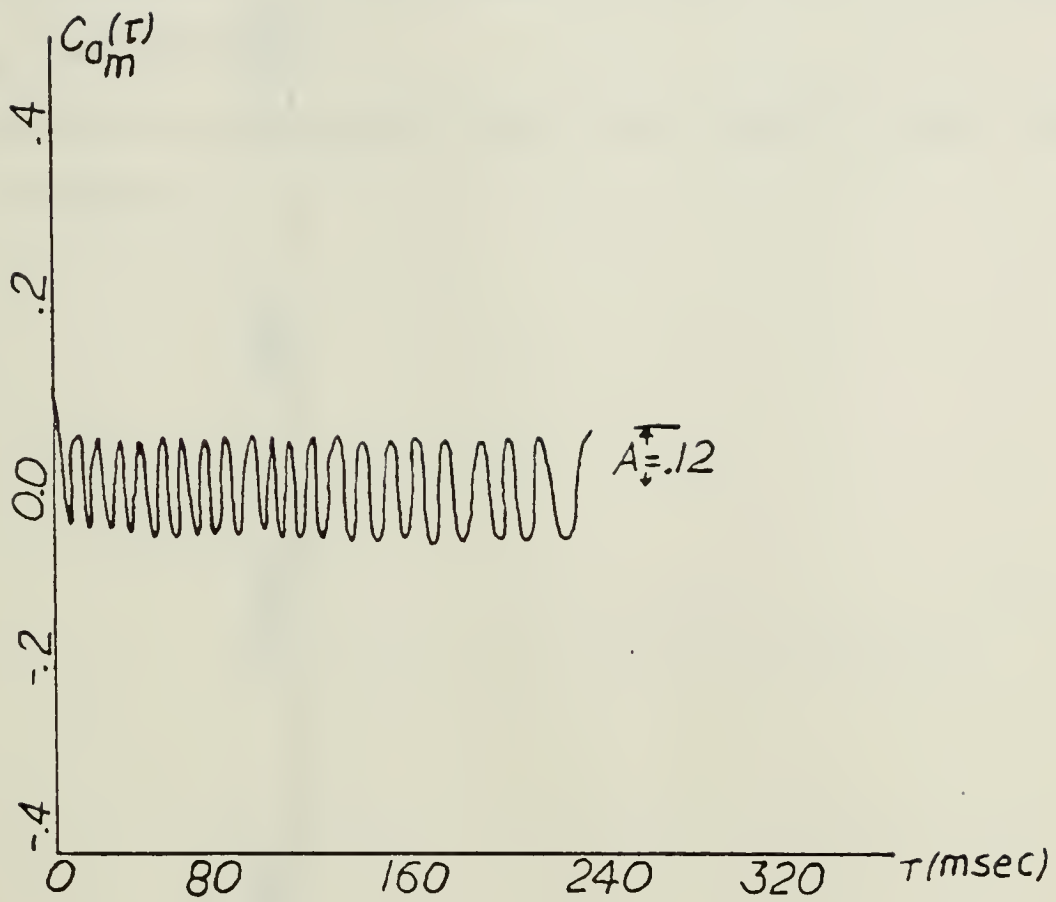
48

Figure 5.1  Cam(τ) with Conical-Scan Modulation
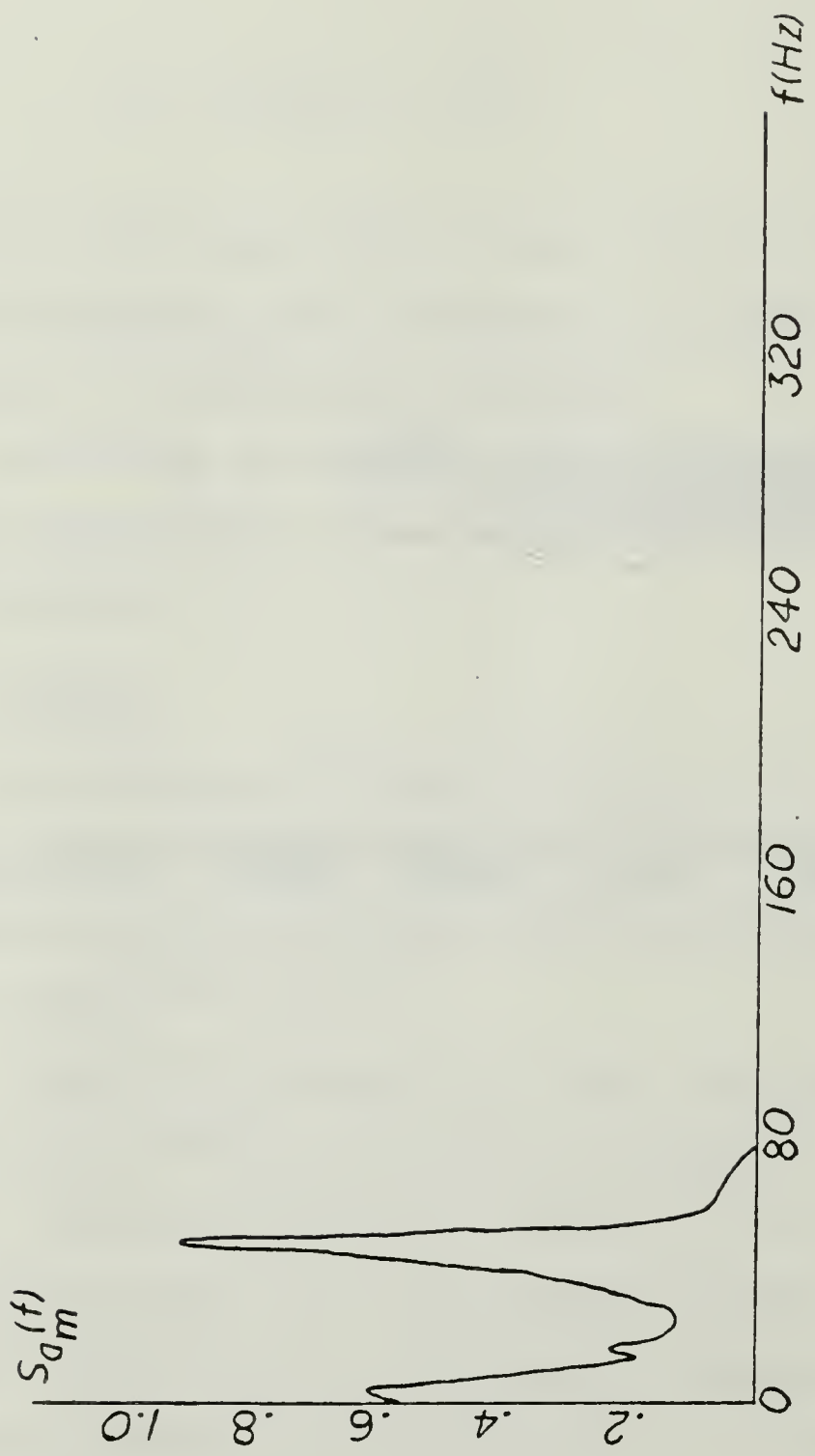
49

Figure 5.2 Spectral Density of Amplitude

50

If F = 33 Hz then, since Sz(f) has been normalized, the height of the main peak at $f_b$ is 1.0 as shown in Fig. 5.3. Thus expect by (5-2) that there should be two secondary peaks of height Ds = 0.06 added to Sz(f) at $f + f_s$ and $f - f_s$, respectively.

As may be seen in the figure the results agree well with what we expect.
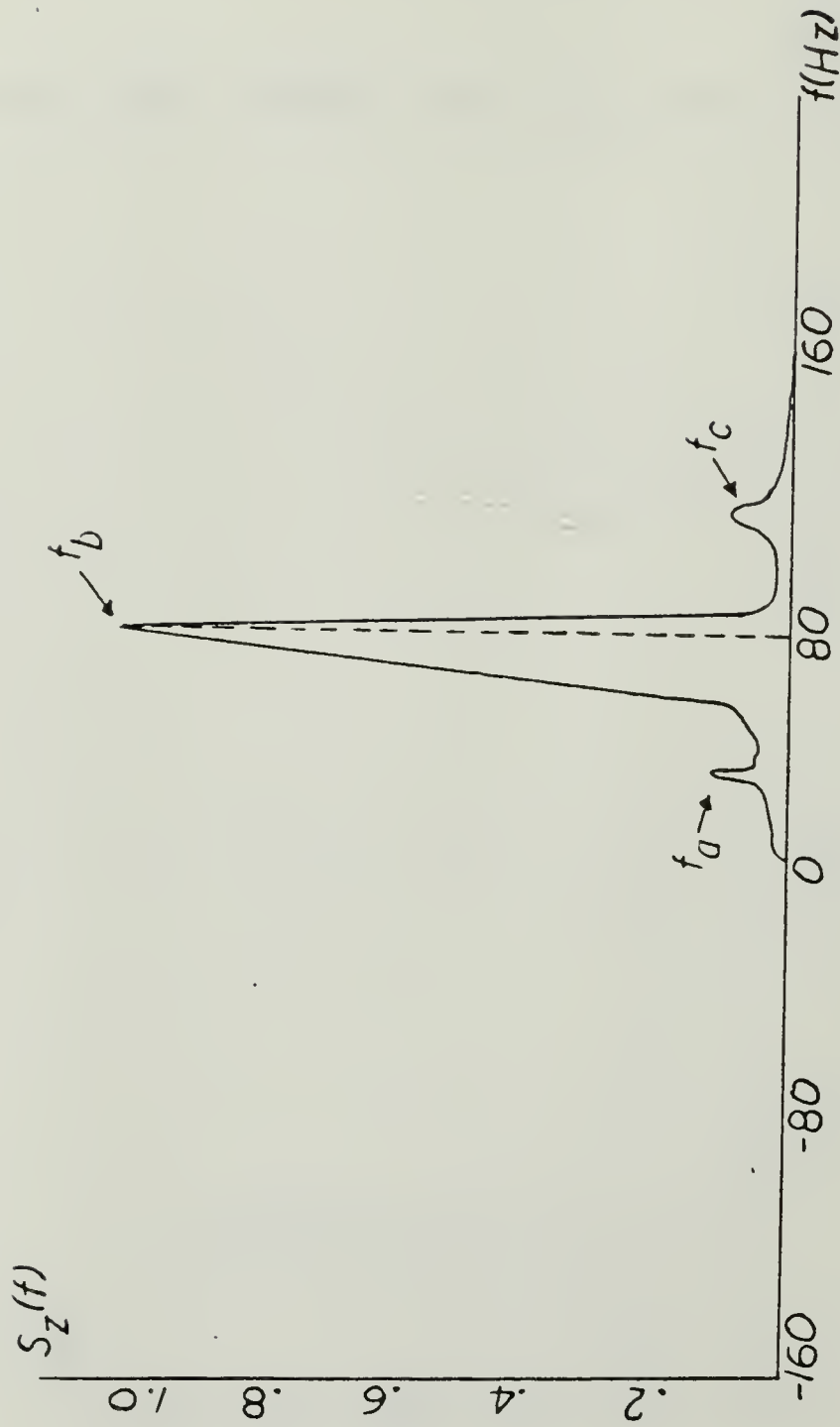
51

Figure 5.3  Sz(f) when Conical-Scan Modulation is Present

## VI.  <u>MODEL SIMULATION</u>

A model missile-ship-chaff has been simulated on a computer program [Ref. 5].  The simulation requires continuous calculation while maintaining the constraint that both ship and chaff remain within the same radar resolution cell.  The simulation must be flexible enough to accommodate ship, chaff and scenario parameters as desired to provide the optimum confusion of the missile.

## A.  INPUT VARIABLES

Input variables needed to describe the ship are its radar cross section and initial range from the radar of the missile.  The ship RCS (Radar Cross Section) will be assumed constant, to be specified by the user prior to simulation. For example, one can specify the average RCS over all aspect angles.  Since the model assumes that the ship has constant RCS it is possible to vary while the simulation is in progress.

Input variables to describe the radar of missile is a 10 GHz X-band, pulsed radar with the following range specifications:  1) Maximum free space range is to be 40 km; 2) Minimum range should be 10 km; 3) Maximum unambiguous range should be at least equal to the maximum free space range.

B.  TECHNICAL PARAMETERS

Known technical parameters for the radar follow:

1)  Transmitter

- Operating frequency is 10 GHz.

- Wavelength is 0.03 meters.

- Maximum power available is 250 kw.

- Duty cycle is 0.004.

2)  Receiver

- Receiver operates at standard temperature.

- Post-detection integration occurs in the receiver on all pulses lying in the 3 db beamwidth.

3)  Targets - Targets are Swerling Case II with radar cross section as follows:

- Ship = 5000 $m^2$

- Chaff = 10000 $m^2$

- Probability of detection is to be 90 percent.

4)  Losses

- Processing:  2 dB

- Beam Shaping :  1 dB

- No others.

Input variables to describe the chaff are RCS backscatter coefficient, height of chaff.  After chaff is dispended for a few seconds the dipoles have some agitation that depend on the type of cartridge which has been used, then the term "new" chaff is referred to in this state. After a lot of time, only naturally occurring winds affect

54

the chaff dipoles; in this situation use the term "mature" chaff. The methods which are used to collect new-chaff and mature-chaff data are different in some way.

Because of the random motion of the dipoles these tend to cause a chaff cloud to grow with time. However, little quantitive information is available on chaff cloud size as a function of time and no attempt was made to measure chaff cloud dimensions during simulation.

An improved type of discrete chaff unit is the chaff cartridge which is a cylinder packed with aluminum-coated glass fibers and fired much like a shotgun shell.

C. "NEW" CHAFF DATA

To obtain new-chaff data, a leading range gate was positioned on the dispensing cartridge producing a chaff cloud the same as a wake. There are trailing gates positioned behind the leading gate received echoes from the new chaff. Based on this information, the chaff cloud is contained entirely within the radar beam.

D. "MATURE" CHAFF DATA

To obtain mature-chaff data, the range gate selected for recording was positioned at the range of the chaff cloud and the echo signal received in the gate was recorded for several seconds. For mature-chaff data the chaff cloud almost certainly extends beyond the beam since measurements were made minutes after dispensing.

E.  REQUIREMENTS

The previous radar parameters and the discrete unit dispensing method are entered into in this model.  The results of the simulation for new-chaff, mature-chaff clouds and range specifications for the optimum confusion of the missile will be presented below:

1)  Chaff-to-noise-plus clutter ratio (Chaff/N+C) appears in Table II and Figure 6.1 for "new" chaff while Tables III, IV, and Figures 6.2, 6.3 for "mature" chaff.

2)  Signal-to-noise-plus clutter ratio (S/N+C) appears in Tables V, VI, VII, and Figures 6.4, 6.5, and 6.6.

3)  Chaff/N+C and S/N+C comparison appears in Figures 6.7, 6.8, and 6.9.  In those figures the section of the curves shows the effective distance in which the missile is confused.

# TABLE II

## CHAFF/N+C VALUES VS. CHAFF-MISSILE DISTANCE (NEW CHAFF)

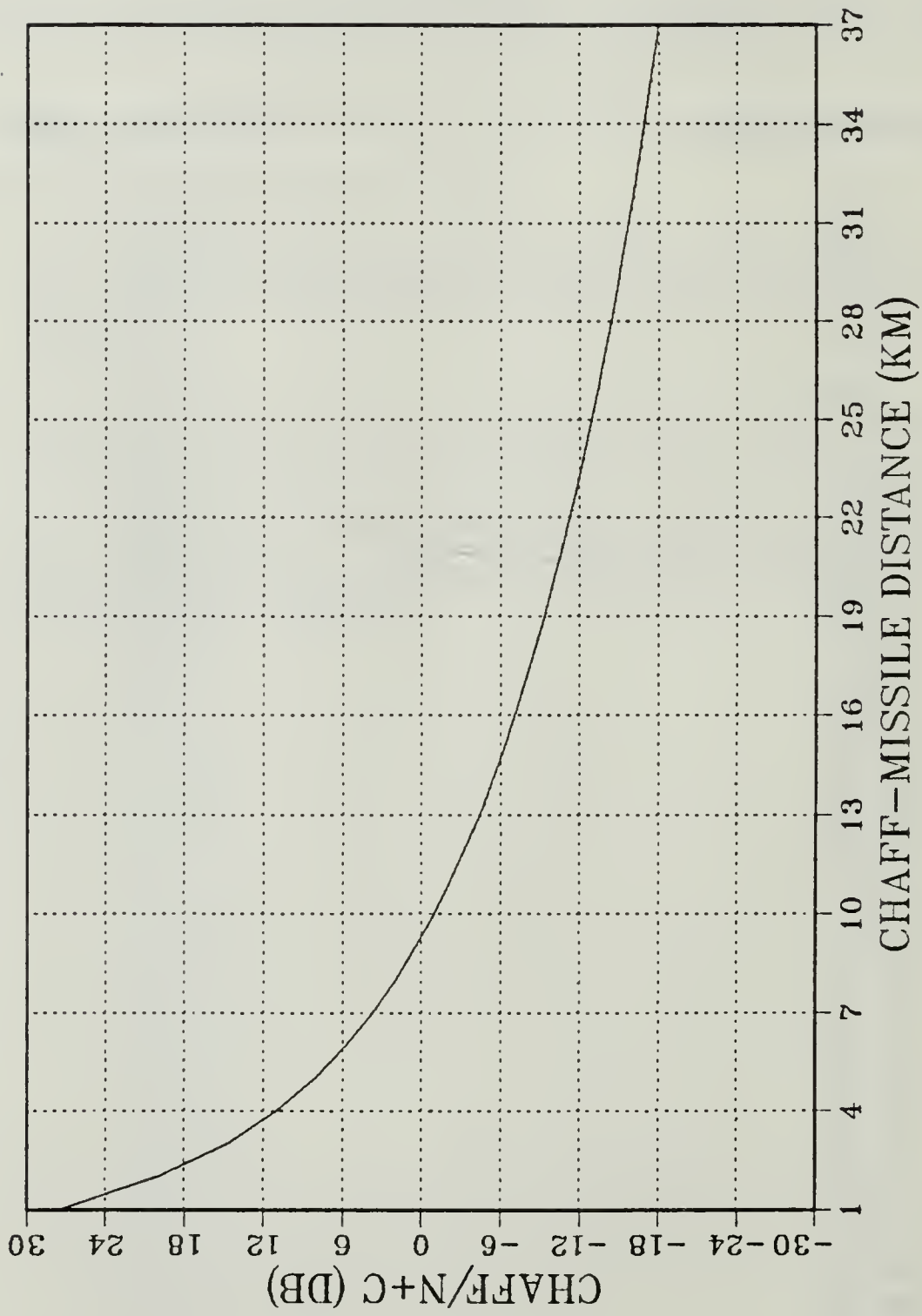| Distance (km) | Chaff/N+C (db) |
|---|---|
| 1.00 | 27.613 |
| 2.00 | 20.046 |
| 3.00 | 14.762 |
| 4.00 | 11.014 |
| 5.00 | 8.106 |
| 6.00 | 5.731 |
| 7.00 | 3.722 |
| 8.00 | 1.982 |
| 9.00 | 0.448 |
| 10.00 | -0.925 |
| 11.00 | -2.167 |
| 12.00 | -3.300 |
| 13.00 | -4.343 |
| 14.00 | -5.309 |
| 15.00 | -6.208 |
| 16.00 | -7.049 |
| 17.00 | -7.838 |
| 18.00 | -8.583 |
| 19.00 | -9.288 |
| 20.00 | -9.956 |
| 21.00 | -10.592 |
| 22.00 | -11.198 |
| 23.00 | -11.777 |
| 24.00 | -12.331 |
| 25.00 | -12.863 |
| 26.00 | -13.374 |
| 27.00 | -13.866 |
| 28.00 | -14.340 |
| 29.00 | -14.797 |
| 30.00 | -15.239 |
| 31.00 | -15.666 |
| 32.00 | -16.080 |
| 33.00 | -16.480 |
| 34.00 | -16.869 |
| 35.00 | -17.247 |
| 36.00 | -17.614 |
| 37.00 | -17.971 |

Figure 6.1  Chaff to Noise Plus Clutter Ratio vs. Chaff-Missile Distance (New Chaff)

## TABLE III

### CHAFF/N+C VALUES VS. CHAFF-MISSILE DISTANCE (MATURE CHAFF)

| Distance (km) | Chaff/N+C (db) |
|---|---|
| 1.00 | 26.178 |
| 2.00 | 17.145 |
| 3.00 | 11.861 |
| 4.00 | 8.113 |
| 5.00 | 5.206 |
| 6.00 | 2.830 |
| 7.00 | 0.822 |
| 8.00 | -0.918 |
| 9.00 | -2.453 |
| 10.00 | -3.825 |
| 11.00 | -5.067 |
| 12.00 | -6.201 |
| 13.00 | -7.244 |
| 14.00 | -8.209 |
| 15.00 | -9.108 |
| 16.00 | -9.949 |
| 17.00 | -10.739 |
| 18.00 | -11.484 |
| 19.00 | -12.188 |
| 20.00 | -12.856 |
| 21.00 | -13.492 |
| 22.00 | -14.098 |
| 23.00 | -14.677 |
| 24.00 | -15.232 |
| 25.00 | -15.764 |
| 26.00 | -16.275 |
| 27.00 | -16.766 |
| 28.00 | -17.240 |
| 29.00 | -17.697 |

TABLE IV

CHAFF/N+C VALUES VS. CHAFF-MISSILE DISTANCE (MATURE CHAFF)

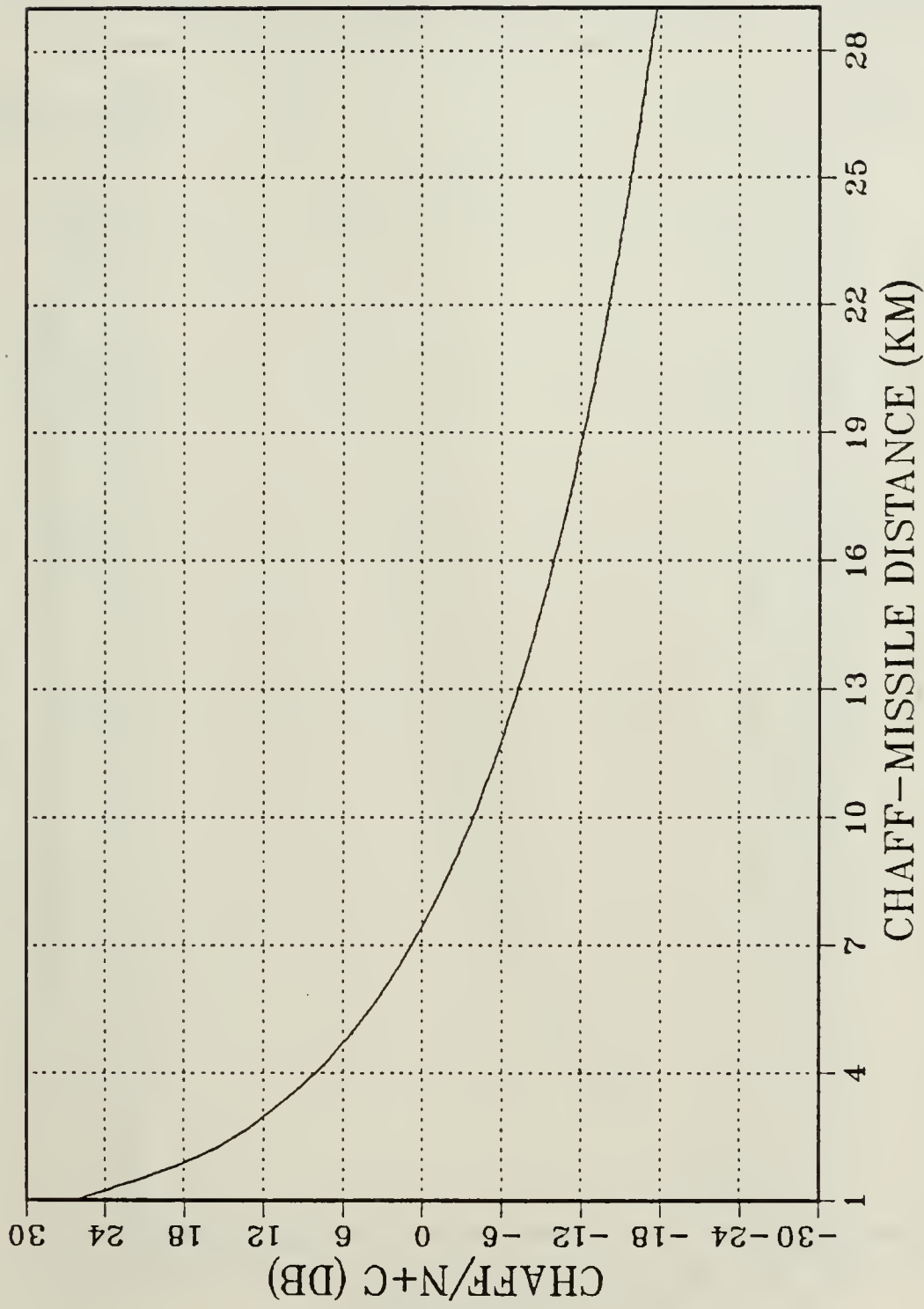| Distance (km) | Chaff/N+C (db) |
|---|---|
| 1.00 | 23.166 |
| 2.00 | 14.134 |
| 3.00 | 8.851 |
| 4.00 | 5.103 |
| 5.00 | 2.195 |
| 6.00 | -0.180 |
| 7.00 | -2.189 |
| 8.00 | -3.928 |
| 9.00 | -5.463 |
| 10.00 | -6.836 |
| 11.00 | -8.077 |
| 12.00 | -9.211 |
| 13.00 | -10.254 |
| 14.00 | -11.220 |
| 15.00 | -12.118 |
| 16.00 | -12.959 |
| 17.00 | -13.749 |
| 18.00 | -14.494 |
| 19.00 | -15.198 |
| 20.00 | -15.867 |
| 21.00 | -16.502 |
| 22.00 | -17.108 |

# MATURE CHAFF



Figure 6.2 Chaff to Noise Plus Clutter Ratio vs. Chaff-Missile Distance (Mature Chaff)
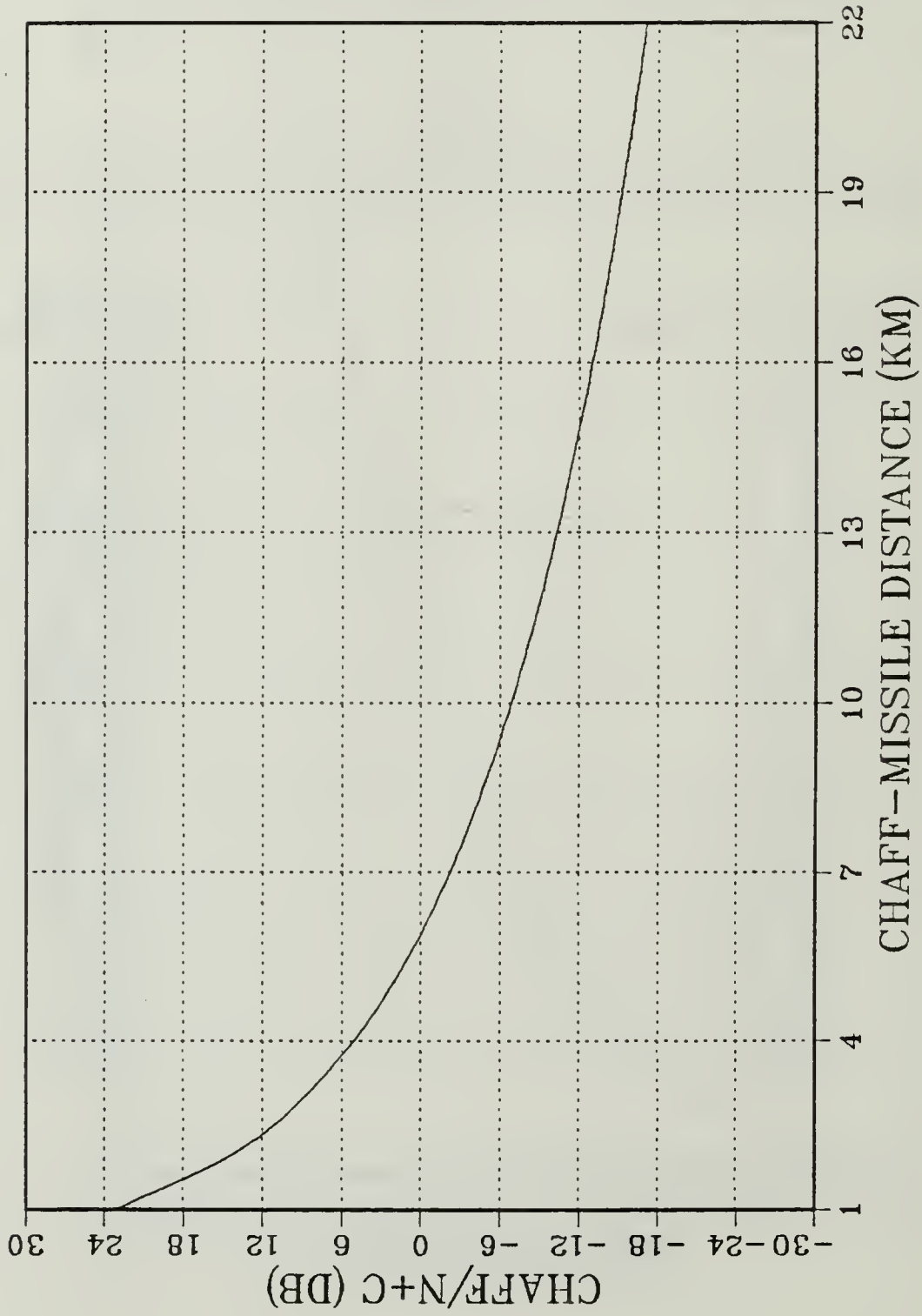
# MATURE CHAFF



Figure 6.3  Chaff to Noise Plus Clutter Ratio vs. Chaff-Missile Distance (Mature Chaff)

62

# TABLE V

## S/N+C VALUES VS. SHIP-MISSILE DISTANCE (NEW CHAFF)

| Distance (km) | S/N+C (db) |
|---|---|
| 1.00 | 4.507 |
| 2.00 | 1.508 |
| 3.00 | -0.2508 |
| 4.00 | -1.499 |
| 5.00 | -2.468 |
| 6.00 | -3.259 |
| 7.00 | -3.929 |
| 8.00 | -4.509 |
| 9.00 | -5.020 |
| 10.00 | -5.478 |
| 11.00 | -5.892 |
| 12.00 | -6.269 |
| 13.00 | -6.617 |
| 14.00 | -6.939 |
| 15.00 | -7.239 |
| 16.00 | -7.519 |
| 17.00 | -7.782 |
| 18.00 | -8.030 |
| 19.00 | -8.265 |
| 20.00 | -8.488 |
| 21.00 | -8.700 |
| 22.00 | -8.902 |
| 23.00 | -9.095 |
| 24.00 | -9.280 |
| 25.00 | -9.457 |
| 26.00 | -9.627 |
| 27.00 | -9.791 |
| 28.00 | -9.949 |
| 29.00 | -10.100 |
| 30.00 | -10.240 |
| 31.00 | -10.391 |
| 32.00 | -10.520 |
| 33.00 | -10.660 |
| 34.00 | -10.790 |
| 35.00 | -10.910 |
| 36.00 | -11.040 |
| 37.00 | -11.160 |

# TABLE VI

## S/N+C VALUES VS. SHIP-MISSILE DISTANCE (MATURE CHAFF)

| Distance (km) | S/N+C (db) |
|:---:|:---:|
| 1.00 | 4.516 |
| 2.00 | 1.510 |
| 3.00 | -0.250 |
| 4.00 | -1.500 |
| 5.00 | -2.467 |
| 6.00 | -3.260 |
| 7.00 | -3.929 |
| 8.00 | -4.509 |
| 9.00 | -5.020 |
| 10.00 | -5.478 |
| 11.00 | -5.892 |
| 12.00 | -6.269 |
| 13.00 | -6.617 |
| 14.00 | -6.939 |
| 15.00 | -7.238 |
| 16.00 | -7.519 |
| 17.00 | -7.782 |
| 18.00 | -8.030 |
| 19.00 | -8.265 |
| 20.00 | -8.488 |
| 21.00 | -8.700 |
| 22.00 | -8.902 |
| 23.00 | -9.095 |
| 24.00 | -9.280 |
| 25.00 | -9.457 |
| 26.00 | -9.627 |
| 27.00 | -9.791 |
| 28.00 | -9.949 |
| 29.00 | -10.102 |

# TABLE VII

## S/N+C VALUES VS. SHIP-MISSILE DISTANCE (MATURE CHAFF)

| Distance (km) | S/N+C (db) |
|---|---|
| 1.00 | 4.519 |
| 2.00 | 1.511 |
| 3.00 | -0.250 |
| 4.00 | -1.498 |
| 5.00 | -2.467 |
| 6.00 | -3.259 |
| 7.00 | -3.929 |
| 8.00 | -4.509 |
| 9.00 | -5.020 |
| 10.00 | -5.478 |
| 11.00 | -5.892 |
| 12.00 | -6.269 |
| 13.00 | -6.617 |
| 14.00 | -6.939 |
| 15.00 | -7.238 |
| 16.00 | -7.519 |
| 17.00 | -7.782 |
| 18.00 | -8.030 |
| 19.00 | -8.265 |
| 20.00 | -8.488 |
| 21.00 | -8.700 |
| 22.00 | -8.902 |

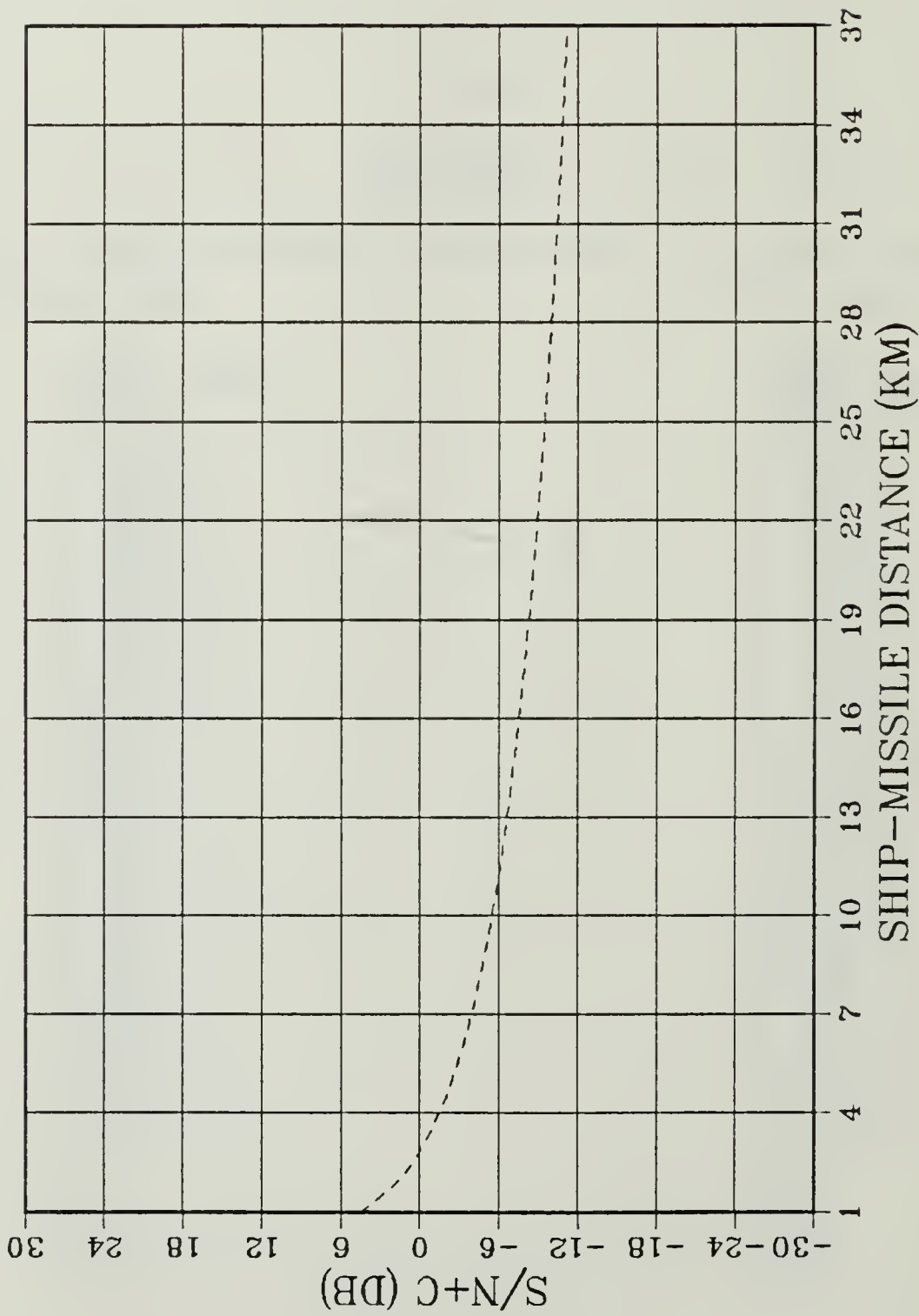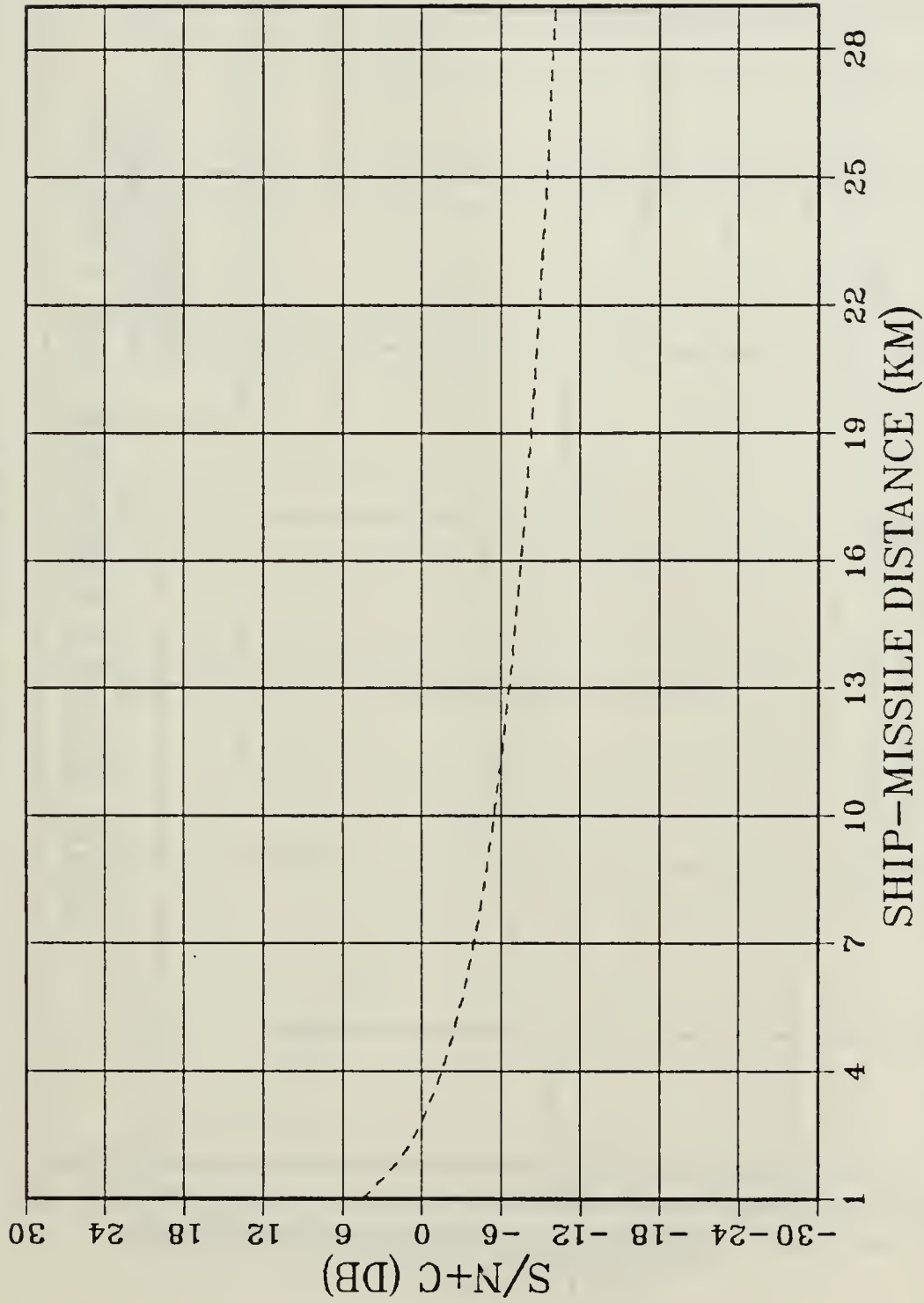Figure 6.4  Signal to Noise Plus Clutter Ratio vs. Ship-Missile Distance (New Chaff)

66

Figure 6.5   Signal to Noise Plus Clutter Ratio vs. Ship-Missile Distance
(Mature Chaff)

# MATURE CHAFF
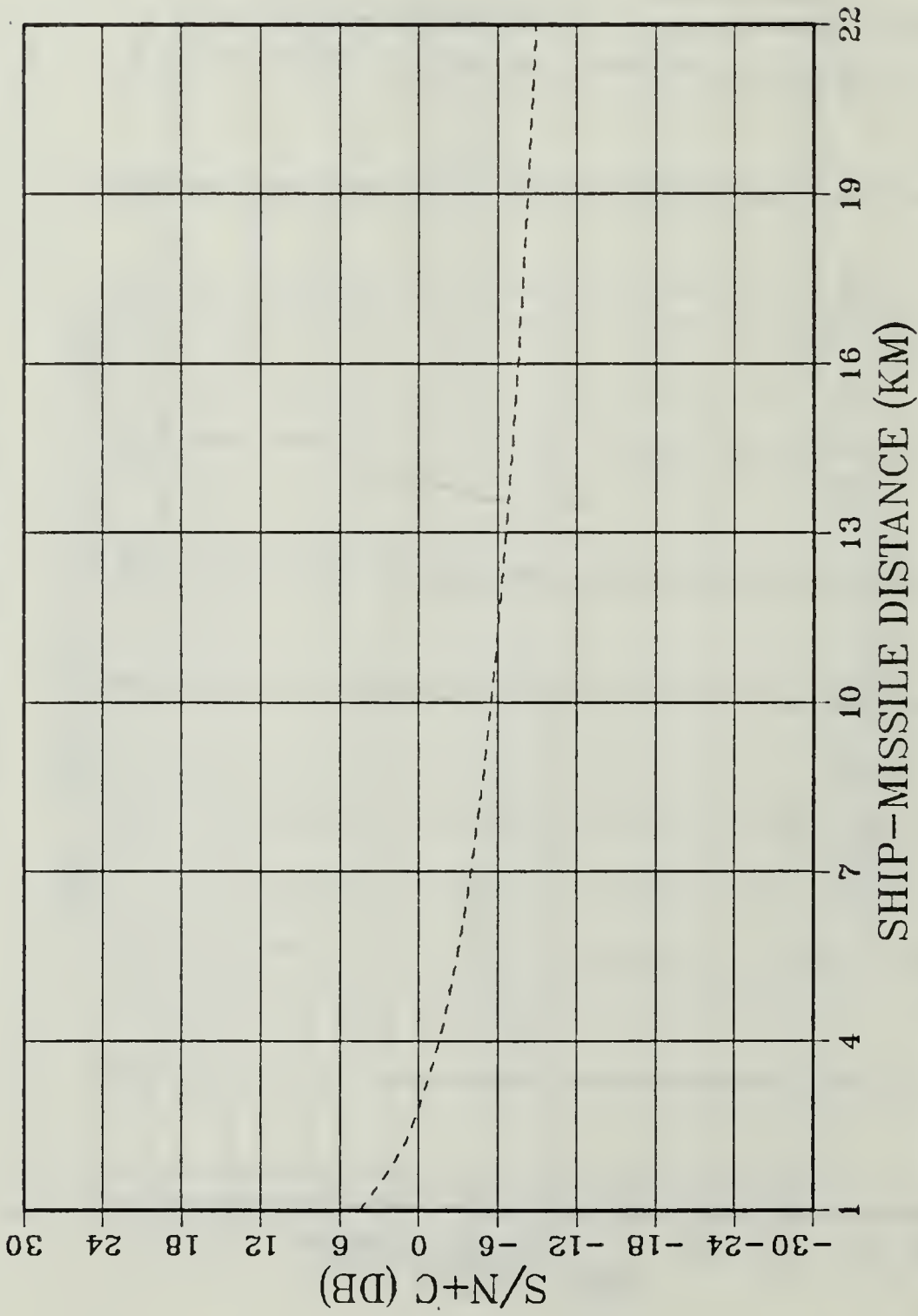


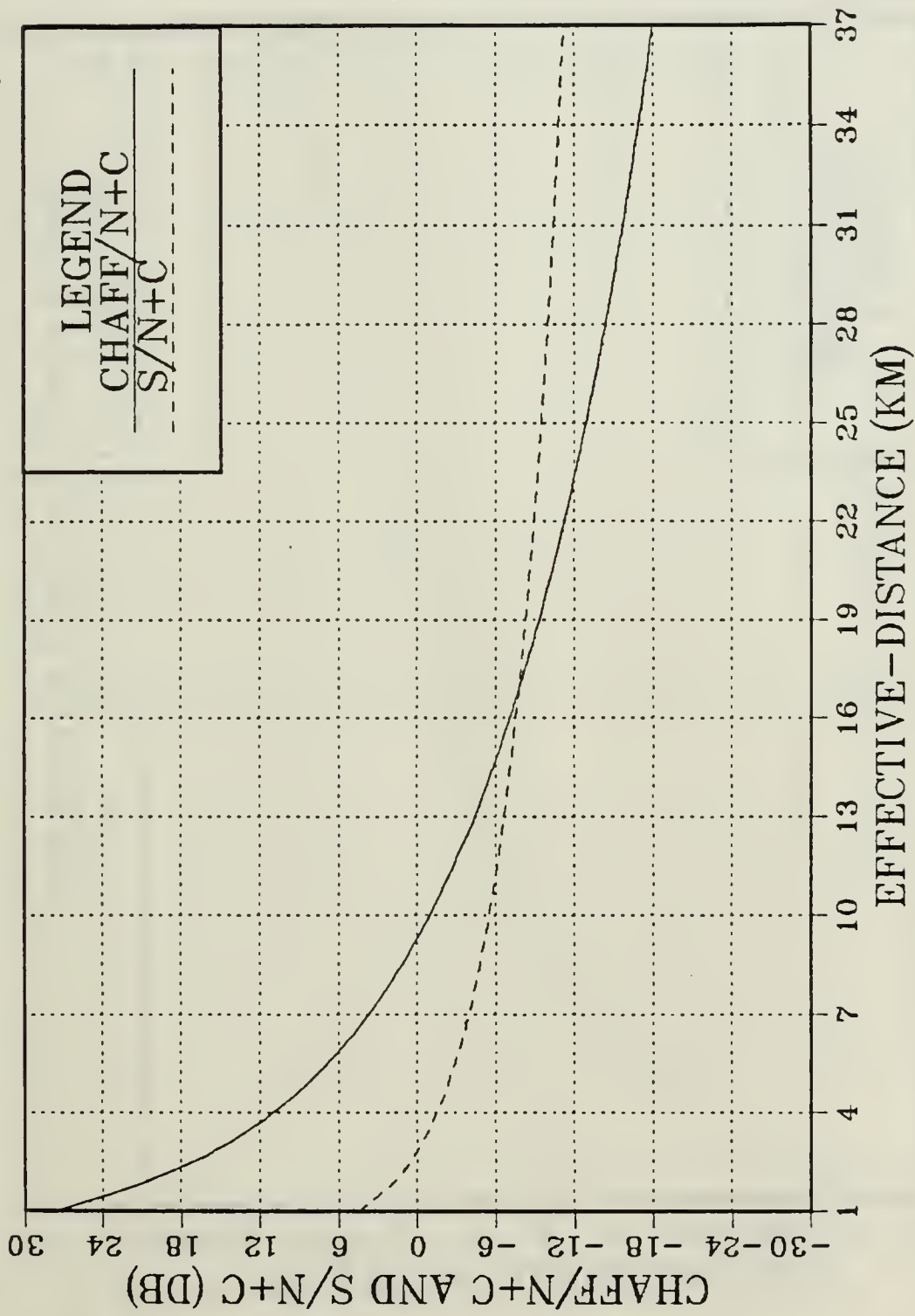Figure 6.6 Signal to Noise Plus Clutter Ratio vs. Ship-Missile Distance (Mature Chaff)

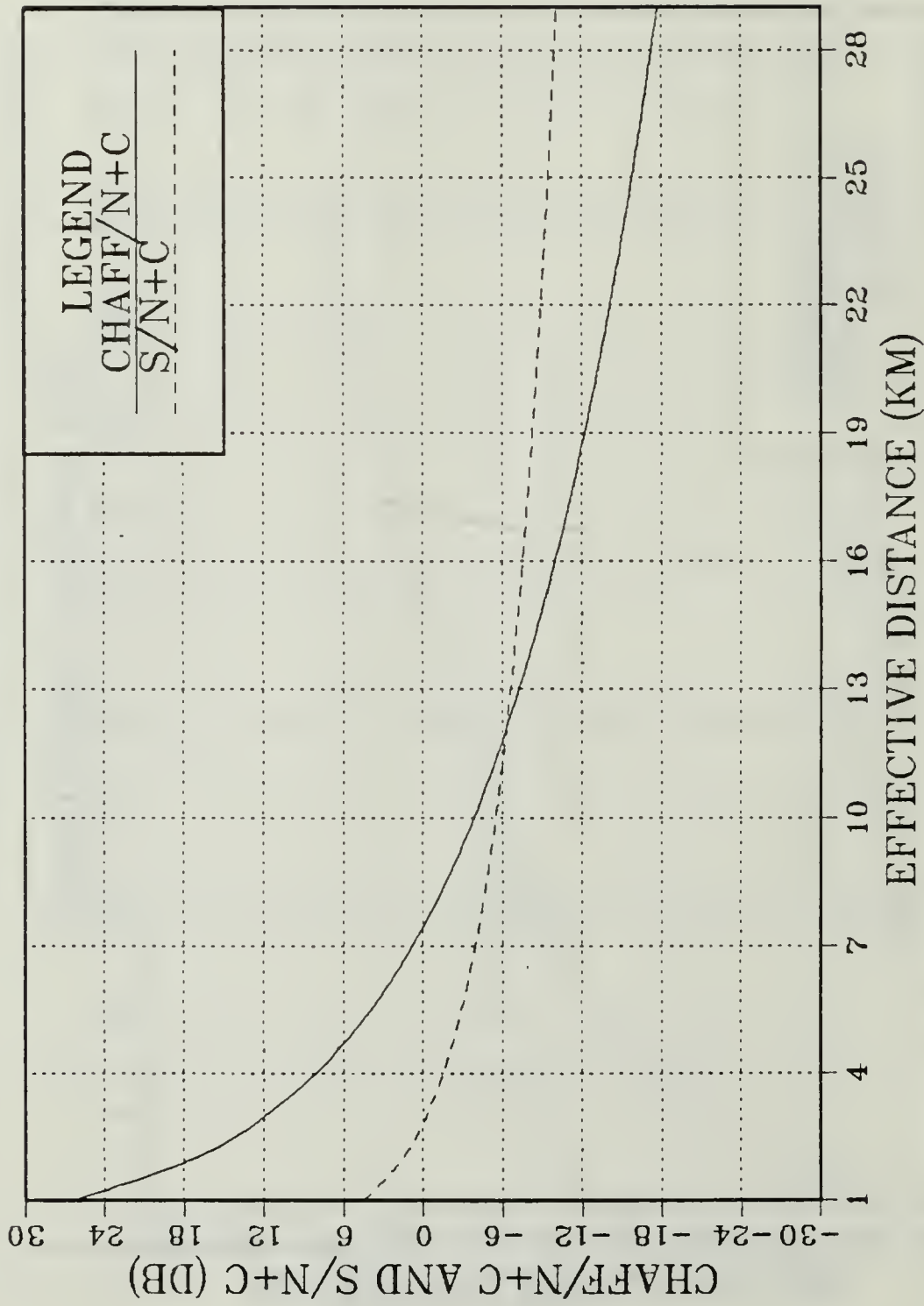Figure 6.7  Chaff/N+C and S/N+C Comparison vs. Distance (New Chaff)

69

Figure 6.8 Chaff/N+C and S/N+C Comparison vs. Distance (Mature Chaff)
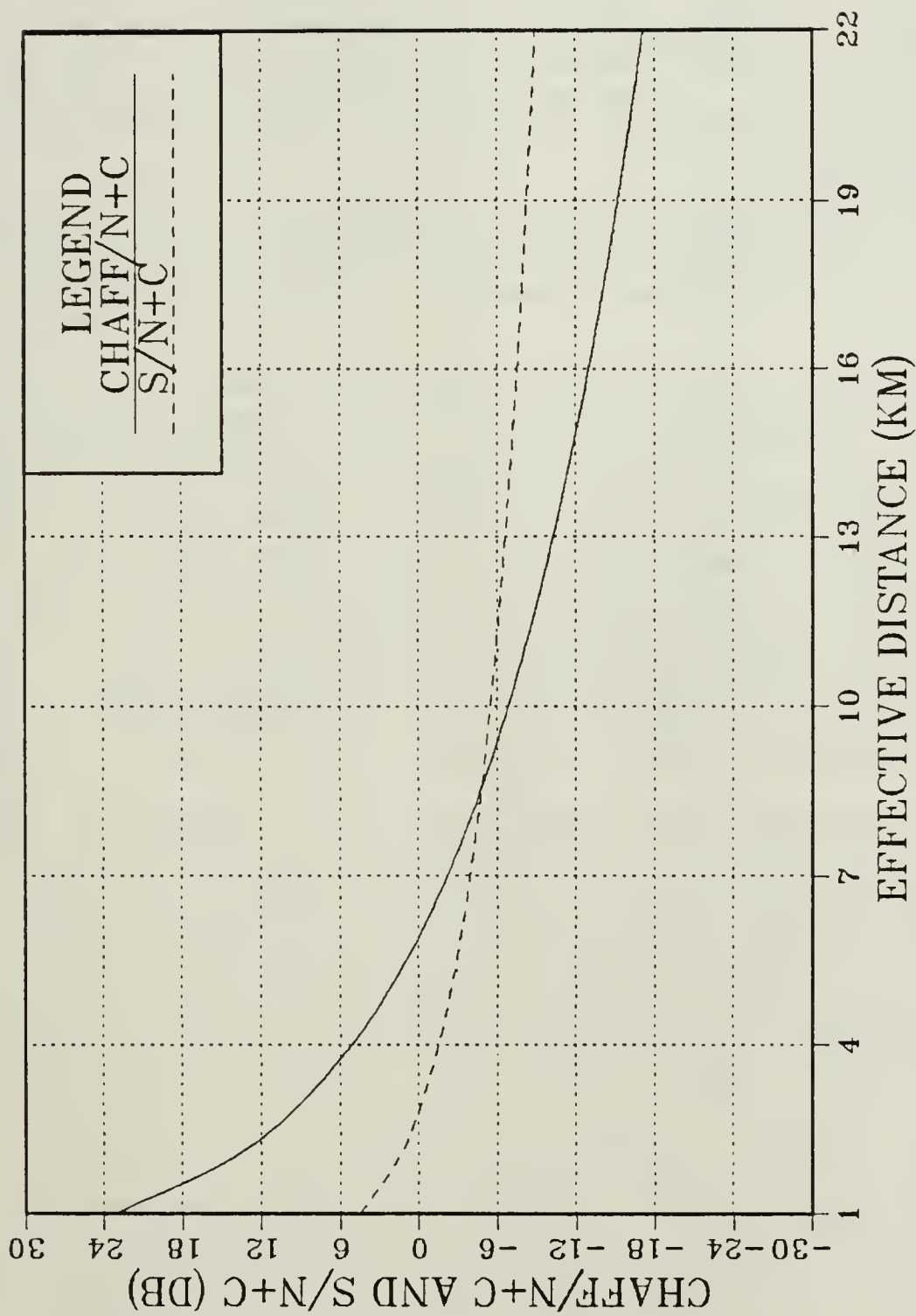
70

Figure 6.9   Chaff/N+C and S/N+C Comparison vs. Distance (Mature Chaff)

# VII.   CONCLUSIONS

Maximizing the effectiveness of chaff, in a self-
protective role, is one method to increase the survivability
of combat ships.

This thesis has produced a simulation that allows the
user to study how the parameters induce the optimum
confusion.

The most dominant factor in chaff effectiveness is the
radar cross section of the chaff compared to the ship at the
time when ship and chaff are in the same resolution cell.

The simulation created in Section VI utilizes this
factor and this constraint increases chaff effectivenss.

In Figure 6.1 we see the decreasing effectiveness of
chaff of a given size chaff cloud with increasing range.
This is for the case of the chaff cloud immediately after
the chaff burst.  Figures 6.2 and 6.3 display the
effectiveness of chaff as a function of range for a mature
chaff cloud.  That is, one that has been in existence for
several minutes.  Figure 6.3 is for a larger radar cross
section chaff cloud.  Figure 6.4 displays essentially the
signal to noise plus chaff ratio as a function of range for
a given radar cross section of ship.  In the examples shown,
the effectiveness of the chaff would be very good in

decoying a missile from the ship in that the signal to chaff ratio is less than one throughout the flight until approximately 3 kilometers of range. Figure 6.5 is similar to 6.4 only it now considers a mature chaff cloud as opposed to a new chaff cloud. Figure 6.6 is similar to Figure 6.5 only it involves a larger chaff cloud radar cross section. Figure 6.7 is a composite plot of the chaff to noise plus signal to noise ratio.

This is a composite figure showing the effectiveness of the chaff to clutter ratio and signal to clutter ratio as a function of the range. The critical point to observe is when the signal to clutter ratio intersects the chaff to clutter ratio. One may then become concerned regarding the missile radar swinging to track the signal as opposed to the chaff.

In this figure, it indicates that the critical range is at approximately 16 kilometers. In Figure 6.8 we have a similar plot only here showing a mature chaff cloud. The critical range occurs at approximately 12 kilometers. In Figure 6.9 we have again the comparison of signal and chaff clutter ratios. Here the critical range in relative ratios occurs at approximately 9 kilometers. These figures and the simulations which produce them give considerable insight into the effectiveness of the chaff defense against the ASCM.

From such plots as these one can conclude such things as
whether or not multiple chaff bursts are necessary to
increase the chaff radar cross-section or whether a
different angle of aspect between the ship and incoming
missile is necessary to reduce the ships radar cross section
to thereby increase the chaff's effectiveness over the
ship's radar cross section.  Out of such simulations as
these, one concludes the timeliness of very rapid reaction
in terms of chaff deployment.  That is, the sooner one can
obtain a mature cloud larger than the ship, the better.

APPENDIX

CONICAL SCAN MODULATION FUNCTION

In this appendix an appropriate expression for m(t) based on the assumptions (Section V) is obtained.

Let $z_m(t)$ and $z(t)$ denote the received complex envelope signals with and without conical-scan modulation, respectively. Then the signal without modulation is the sum of echoes from K dipoles in the range cell [Ref. 4].

$$z(t) = \sum_{k=1}^{K} a_k \exp[2nf_K t + r_K]$$

So for Kth dipole the parameters $a_K$, $r_K$, and $f_K$ depend on the range and radial velocity of dipole.

An expression can be generated to modify the above expression to include modulation functions $m_K(t)$ which account for the varying strengths of echoes from the dipoles due to changing beam position [Ref. 4]:

$$z_m(t) = \sum_{K=1}^{K} m_K(t) a_K \exp[jd_K] \qquad (A-1)$$

75

where:

$$d_K = 2nf_K t + r_K$$

If the assumptions (Section V) are true and the dipoles are not widely dispersed then the modulation functions $m_K(t)$ will be approximately equal to a common modulation function $m(t)$.

So (A-1) simplified to:

$$z_m(t) = m(t) \sum_{K=1}^{K} a_K \exp[jd_K] = m(t)z(t) = m(t)a(t)\exp[jd(t)]$$

(A-2)

From equation (A-2) $z_m(t)$ is equal to $z(t)$ multiplied by a real-valued modulation function $m(t)$ which is periodic at the scan frequency. Thus the amplitude of $z_m(t)$ given by $a_m(t) = m(t)a(t)$ where $a(t)$ is the amplitude of $z(t)$. Because $m(t)$ is periodic it can be written as Fourier series with scan frequency $f_s$ [Ref. 4]:

$$m(t) = Mo + \sum_{K=1}^{K} M_K \cos(2nKf_s t + a_K)$$

(A-3)

Suppose $Ca(t)$ and $Cam(t)$ denote the timer-average autocovariance functions of $a(t)$ and $a(t)$ respectively, then assuming that $Cam(t)$ goes to zero t goes to infinity one may write the following:

76

$$Ca_m(t) = \sum_{K=1}^{K} (M_K^2/2) \cos(2nf_st)(\bar{a})^2 \qquad \text{(A-4)}$$

$$\bar{a}_m = Mo\bar{a} \qquad \text{(A-5)}$$

where:

$\bar{a}_m$, $\bar{a}$:  Time average of $a$ (t) and a(t)

So with a good approximation take Mn=0 for $n \geq 2$ in (A-3) and (A-4).  Thus m(t) may be written as:

$$m(t) = Mo + M_1\cos(2nf_st + a_1) \qquad \text{(A-6)}$$

There is one useful relationship between Mo and $M_1$. From (A-4) and (A-6) $M_1$ is related to the amplitude of the cosine wave of Cam(t) with $M_1^2(a)^2/2 = A$.  Now when this result is combined with the (A-5) we find that $M_1 = BMo$ where:

$$B = (2A/a_m)^{1/2}$$

Since both A and $\bar{a}_m$ are estimated using recorded data then B may be estimated.

So we have found that the modulation function may be approximated by the expression of the form:

$$m(t) = Mo + BMo \cos(2nf_st + a_1)$$

# LIST OF REFERENCES

1. Skolnick, Merrill I., <u>Introduction to Radar Systems</u>, McGraw-Hill, 1980.

2. Van Brunt, Leroy B., <u>Applied ECM</u>, EW Engineering Inc., 1978.

3. Butters, Brian C. F., "Chaff", <u>IEEE Proceedings</u>, Vol. 129, Pt. F, No. 3, June 1982.

4. Flake, Robert H., "Spectral Characteristics of Radar Echoes from Aircraft Dispensed Chaff," <u>IEEE Proceedings</u>, Vol. AES-21, No. 7, January 1985.

5. Skillman, W., <u>Radar Calculation</u>, January 1984.

INITIAL DISTRIBUTION LIST

No. Copies

1. Defense Technical Information Center                    2
   Cameron Station
   Alexandria, Virginia  22304-6145

2. Library, Code 0142                                      2
   Naval Postgraduate School
   Monterey, California 93943-5100

3. Hellenic Navy General Staff                             1
   Geniko Epiteleio Nautikou
   Stratopedo Papagou
   Athens, Greece

4. Professor Harold A. Titus, Code 62Ts                    2
   Department of Electrical and Computer
       Engineering
   Naval Postgraduate School
   Monterey, California 93943-5100

5. Professor Alex Gerba, Jr., Code 62Gz                    1
   Department of Electrical and Computer
       Engineering
   Naval Postgraduate School
   Monterey, California 93943-5100

6. Department Chairman, Code 62Rr                          1
   Department of Electrical and Computer
       Engineering
   Naval Postgraduate School
   Monterey, California 93943-5100

7. LT A. Katsicogiannis                                    3
   Miltiadou 24, Glifada
   Athens, Greece

8. Harilaos Stamelos                                       1
   Iconomou ex Iconomon 30
   Larissa, Greece